INFORMATION TO USERS

This dissertation was produced from a microfilm copy of the original document. While the most advanced technological means to photograph and reproduce this document have been used, the quality is heavily dependent upon the quality of the original submitted.

The following explanation of techniques is provided to help you understand markings or patterns which may appear on this reproduction.

1. The sign or "target" for pages apparently lacking from the document photographed is "Missing Page(s)". If it was possible to obtain the missing page(s) or section, they are spliced into the film along with adjacent pages. This may have necessitated cutting thru an image and duplicating adjacent pages to insure you complete continuity.

2. When an image on the film is obliterated with a large round black mark, it is an indication that the photographer suspected that the copy may have moved during exposure and thus cause a blurred image. You will find a good image of the page in the adjacent frame.

3. When a map, drawing or chart, etc., was part of the material being photographed the photographer followed a definite method in "sectioning" the material. It is customary to begin photoing at the upper left hand corner of a large sheet and to continue photoing from left to right in equal sections with a small overlap. If necessary, sectioning is continued again — beginning below the first row and continuing on until complete.

4. The majority of users indicate that the textual content is of greatest value, however, a somewhat higher quality reproduction could be made from "photographs" if essential to the understanding of the dissertation. Silver prints of "photographs" may be ordered at additional charge by writing the Order Department, giving the catalog number, title, author and specific pages you wish reproduced.

University Microfilms

300 North Zeeb Road
Ann Arbor, Michigan 48106

A Xerox Education Company

COMPUTER SIMULATION OF DATTNER MODE PROPAGATION IN A PLASMA

by

H. Wade Swinford

A Dissertation Submitted to the Faculty of the

DEPARTMENT OF ELECTRICAL ENGINEERING

In Partial Fulfillment of the Requirements
For the Degree of

DOCTOR OF PHILOSOPHY

In the Graduate College

THE UNIVERSITY OF ARIZONA

1 9 7 2

THE UNIVERSITY OF ARIZONA

GRADUATE COLLEGE

I hereby recommend that this dissertation prepared under my direction by H. Wade Swinford

entitled Computer Simulation of Dattner Mode Propagation in a Plasma

be accepted as fulfilling the dissertation requirement of the degree of Doctor of Philosophy

D B Carey — 1/17/72

Dissertation Director — Date

After inspection of the final copy of the dissertation, the following members of the Final Examination Committee concur in its approval and recommend its acceptance:*

D B Carey	1/17/72
Gerry L Johnson	1/18/72
John A. Reagan	1/18/72
Edgar W. Jenkins	1/26/72
Siegfried Kahler	1/28/72
R. L. Call	3/6/72

*This approval and acceptance is contingent on the candidate's adequate performance and defense of this dissertation at the final oral examination. The inclusion of this sheet bound into the library copy of the dissertation is evidence of satisfactory performance at the final examination.

STATEMENT BY AUTHOR

This dissertation has been submitted in partial fulfillment of requirements for an advanced degree at The University of Arizona and is deposited in the University Library to be made available to borrowers under rules of the Library.

Brief quotations from this dissertation are allowable without special permission, provided that accurate acknowledgment of source is made. Requests for permission for extended quotation from or reproduction of this manuscript in whole or in part may be granted by the head of the major department or the Dean of the Graduate College when in his judgment the proposed use of the material is in the interests of scholarship. In all other instances, however, permission must be obtained from the author.

SIGNED: H. Wade Swinford

ACKNOWLEDGMENTS

It is a sincere pleasure for the author to acknowledge his gratitude to his dissertation director, Dr. Robert N. Carlile, for his friendship and guidance during the author's graduate program. The author would like to thank Dr. Velvin R. Watson for his helpful discussions concerning plasma simulation.

The author is deeply grateful to his wife, Adrienne, for her support and encouragement during the course of his graduate program. The author feels extremely fortunate to have Mr. and Mrs. G. Swinford as parents.

This work was supported by the Department of Electrical Engineering, and by the National Science Foundation under Grant GK-10918.

TABLE OF CONTENTS

LIST OF ILLUSTRATIONS

LIST OF ILLUSTRATIONS (Continued)

ABSTRACT

Current models used to study wave propagation in bounded plasmas are limited to small amplitude waves since the equations must be linearized to obtain a solution. The existing models are also limited because they neglect the spread in the thermal velocities of the electrons in the plasma. It is the objective of this work to develop a model which is equally valid in the small amplitude regime and in the large amplitude or nonlinear regime. This model also includes the spread in thermal velocities of the electrons. The new model presented is a computer simulation model in which a digital computer is used to follow the motion of a statistical sampling of the electrons in the plasma.

The cold plasma model and the warm plasma model are derived from basic transport theory. The assumptions necessary to obtain these models are discussed. The cold plasma model and the warm plasma model are applied to the problem of small amplitude wave propagation in a two dimensional plasma in rectangular coordinates. The results of the two solutions are contrasted. The assumptions necessary to obtain these solutions are presented with respect to the range of validity of the solutions.

The general concept of computer simulation is then discussed. Special emphasis is placed on the numerical techniques which are used

to implement the solution on a digital computer. Three criteria necessary for a valid plasma simulation are presented.

The computer simulation model for waves in a bounded plasma is presented. The boundary conditions on the sample electrons and on the electric potential are discussed. The economic advantages in limiting the computer simulation to symmetric wave modes is shown. Obtaining data on the dispersive properties of the modes propagating in the computer simulation plasma is made difficult due to the presence of the thermal and shot noise inherent in the computer simulation model. A simple model for the temporal behavior of a wavevector is proposed. This simple model is used to demonstrate how time autocorrelation of a wavevector facilitates the determination of the frequency associated with a given wavevector.

The computer simulation model is applied to the study of the natural modes of the bounded, two dimensional plasma. Dispersive data are obtained for the surface wave mode and the two lowest order Dattner modes. The results are found to be in good agreement with the warm plasma model. The variation of the electric potential in the direction transverse to the direction of wave propagation is compared with the predictions of the warm plasma model with good qualitative agreement between the two models. The plasma simulation model is extended to the inhomogeneous plasma.

The results obtained from the computer simulation clearly demonstrate the validity of a computer simulation model for investigations of waves in a plasma.

CHAPTER 1

INTRODUCTION

This work describes the development of a computer model for a plasma which is applicable to the investigation of wave propagation in a bounded plasma at microwave frequencies and above. This computer model overcomes many of the difficulties inherent in other commonly used models for bounded plasmas such as the cold plasma model and the so-called warm plasma model.

Trivelpiece [1958] used the cold plasma model to investigate the waves which could propagate on an isotropic, homogeneous plasma column confined by a dielectric tube and enclosed in a cylindrical waveguide. His calculations showed the existence of a set of modes which are called the surface wave modes since the energy in the mode is confined to the interface between the plasma and the bounding dielectric. The fields of these modes vary azimuthally as $\exp(in\theta)$ where n is an integer and θ is the azimuthal coordinate. Because of the azimuthal variation of the fields, the n=0 mode is called the symmetric mode and the n=1 mode is called the dipolar mode. The symmetric mode is a low-pass mode while the dipolar mode and all higher modes are band-pass modes as is shown in Fig. 1.1. As the propagation constant, β, goes to infinity for these modes the angular frequency, ω, approaches $\omega_p/(1 + \varepsilon_r)^{1/2}$ where ω_p is the plasma frequency of the electrons and ε_r is the relative permittivity of the dielectric bounding the plasma. The geometry of the system

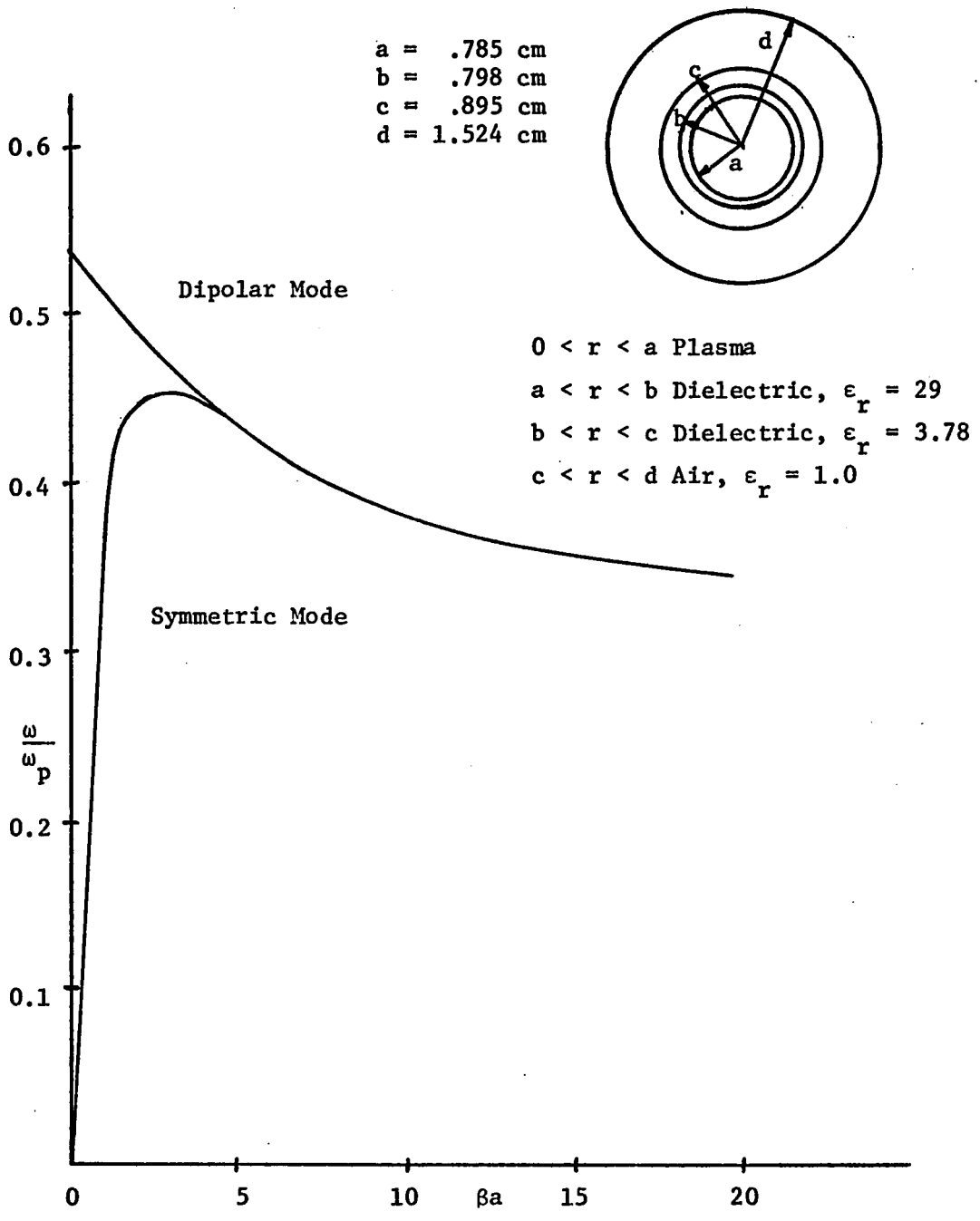

Fig. 1.1 ω-β Diagram of the Symmetric and Dipolar Surface Wave Modes

is shown in the insert of Fig. 1.1. These surface wave modes are the only modes predicted by the cold plasma model.

The surface wave modes have been studied experimentally by several authors. Carlile [1963] as well as Akao and Ida [1964] verified the low-pass and bandpass nature of the symmetric and dipolar modes. The most extensive experimental investigation of the symmetric and dipolar modes is due to Carlile and Swinford [1968]. Their experimental data was compared with theoretical data which was obtained by using a cold plasma model and included the effects of the plasma inhomogeneity and the sheath region which forms at the plasma-dielectric boundary in a real laboratory plasma column. The agreement between theory and experiment was excellent.

In performing their analysis, the above mentioned workers have all used the quasistatic approximation, i.e., $\overline{E} = -\nabla\phi$. Granatstein and Schlesinger [1965] obtained the dispersion relation for surface wave modes again using the cold plasma model for a homogeneous plasma, but without employing the quasistatic approximation.

Crawford [1964] used the cold plasma model and the quasistatic approximation to study the resonance associated with the cut-off frequency (β=0) of the dipolar surface wave mode. This resonance was first described by Tonks [1931]. Rommell [1951] and Dattner [1963] observed experimentally that a plasma column exhibited not one resonance, but a series of resonances. These resonances are called the Dattner-Tonks resonances. The additional resonances which are observed are not predicted by the cold plasma model which neglects the thermal

motion of the electrons. Parker, Nickel, and Gould [1964] were able to predict these resonances using a model of the plasma, called the warm plasma model, which includes first order temperature effects. Their solution accounted for the inhomogeneous electron density and made use of the quasistatic approximation. O'Brien, Gould, and Parker [1965] have shown that these additional resonances are each the cut-off frequency of a propagating mode. These additional warm plasma modes were called the Dattner modes. More recently, the term "Dattner modes" has been extended to include the surface wave modes. Diament, Granatstein, and Schlesinger [1966] have also predicted these modes using the warm plasma model. Their solutions are based on a homogeneous plasma and employ the full set of Maxwell's equations instead of the quasistatic approximation.

The cold plasma model and the warm plasma model have several limitations which are discussed in Chapter 2. These limitations preclude the use of these models in certain engineering applications. In this work a general computer model for the bounded plasma is presented which overcomes the limitations of the cold and warm plasma models. The computer model employs plasma simulation. Some general aspects of plasma simulation are discussed in Chapter 3. Chapter 4 is devoted to the results of the computer experiments performed using the plasma simulation program, and Chapter 5 is the conclusion and suggestions for further work.

CHAPTER 2

PLASMA MODELS

The Kinetic Equation and Distribution Function

A complete specification of the state of a many body system, such as a plasma, necessitates a knowledge of the position and velocity of each of the particles which comprise the system. Since it is impractical to enumerate all these positions and velocities, a statistical approach is adopted. Phase space is a six-dimensional space with three of the axes (x, y, and z) being the position vector components of a particle and the other three axes being the velocity vector components (w_x, w_y, and w_z) of the particle. The complete state of a particle (its position and velocity) is given then as a point in phase space. The state of the system of particles is specified as a set of points in phase space, one point for each particle in the system. As the velocities of the particles change due to acceleration and the positions of the particles change due to their velocities, the representative points in phase space move to reflect the continuously changing state of the system. A statistical description of the system is achieved by defining a phase space distribution function, f. The distribution function is defined such that the product of the distribution function with the differential volume element in phase space, $dx\ dy\ dz\ dw_x\ dw_y\ dw_z$, gives the number of points in phase space within the differential volume.

The differential volume in configuration space, dx dy dz, will be abbreviated as $d^3\bar{r}$ while the differential volume in velocity space will be abbreviated as $d^3\bar{w}$. The differential volume in phase space can then be written as $d^3\bar{r}d^3\bar{w}$. The distribution function is, in general, a function of the six coordinates of phase space as well as time. A knowledge of the distribution function enables one to compute any macroscopic property of the system, such as the number density, the average velocity, or the kinetic energy. For example, the number density, n, is obtained as the integration of the distribution function over all velocities,

$$n(\bar{r},t) = \iiint_{-\infty}^{\infty} f \, d^3\bar{w} \quad . \tag{2.1}$$

The average velocity, which shall be denoted by $\bar{v}$, is given by

$$\bar{v} = \frac{1}{n} \iiint_{-\infty}^{\infty} \bar{w} \, f \, d^3\bar{w} \quad . \tag{2.2}$$

In general, the average of any quantity, Q, is given by

$$\langle Q \rangle = \frac{1}{n} \iiint_{-\infty}^{\infty} Q \, f \, d^3\bar{w} \quad , \tag{2.3}$$

where $\langle Q \rangle$ signifies the average of Q. If a system is composed of several different species of particles, there is a distribution function for each species, for example in a completely ionized gas, there would be a

distribution function for electrons and one distribution function for each specie of ions.

The distribution function, f, is found by solving an equation known as Boltzmann's equation. Boltzmann's equation describes the time dependence of the distribution function and states that the total time rate of change of f is due to the effect of collisions. Boltzmann's equation can be written as

$$\frac{\partial f}{\partial t} + \overline{w} \cdot \nabla_r f + \frac{\overline{F}}{m} \cdot \nabla_w f = B_{coll} \qquad (2.4)$$

where m is the mass of the particle, $\overline{F}$ is the force acting on a particle exclusive of forces due to binary collisions, and B_{coll} describes the effect on the distribution function due to binary collisions. ∇_r is the gradient operator in configuration space,

$$\nabla_r \equiv \hat{x} \frac{\partial}{\partial x} + \hat{y} \frac{\partial}{\partial y} + \hat{z} \frac{\partial}{\partial z} \quad ,$$

and

$$\nabla_w$$

is a gradient operator in velocity space,

$$\nabla_w \equiv \hat{i} \frac{\partial}{\partial w_x} + \hat{j} \frac{\partial}{\partial w_y} + \hat{k} \frac{\partial}{\partial w_z}$$

and

$$\hat{i}, \hat{j}, \text{ and } \hat{k}$$

are unit vectors along the w_x, w_y, and w_z axes respectively. In the laboratory plasma columns of interest in this work one finds that the mean free path for an electron is several times larger than the dimensions of the discharge tube itself. Therefore, an accurate description of the electron gas can be obtained by neglecting the collisions of the electrons. In terms of the Boltzmann equation for the electron distribution function this means that B_{coll} is zero. Then we have

$$\frac{\partial f}{\partial t} + \bar{w} \cdot \nabla_r f + \frac{\bar{F}}{m} \cdot \nabla_w f = 0 \qquad (2.5)$$

as the equation which must be solved to obtain the electron distribution function, f. This collisionless form of Boltzmann's equation is termed the Vlasov equation.

The Moment Equations

In the investigation of the interaction between a plasma and a microwave field one is most interested in the spatial and temporal behavior of the electron number density, n, and the average velocity, $\bar{v}$. These are macroscopic properties of the plasma which may be computed if the distribution function of the system is known.

The solution of Vlasov's equation to obtain the distribution function is often difficult if not impossible and so an alternate method of calculating the macroscopic parameters of the system is desirable. Equations describing these macroscopic variables are obtainable by a process known as taking moments of the Vlasov equation. To compute the

moments one multiplies Vlasov's equation by an arbitrary function of velocity and time, $A(\bar{w},t)$, and integrates each term of the equation over all velocity space. One obtains the general result

$$\frac{\partial}{\partial t}\left(n\langle A\rangle\right) + \nabla_r \cdot \left(n\langle \bar{w}A\rangle\right) - n\left\langle \frac{\bar{F}}{m} \cdot \nabla_w A\right\rangle = 0. \qquad (2.6)$$

The first moment equation is obtained by letting A = 1. One obtains the continuity equation

$$\frac{\partial n}{\partial t} + \nabla_r \cdot (n\bar{v}) = 0 \ . \qquad (2.7)$$

The second moment equation is called the equation of momentum transfer and is obtained by taking $A = \bar{w}$. The result is

$$nm\frac{d\bar{v}}{dt} = qn\ (\bar{E} + \bar{v} \times \bar{B}) - \nabla_r \cdot \bar{\bar{\psi}}\ , \qquad (2.8)$$

where it has been assumed that the force, $\bar{F}$, was $q(\bar{E} + \bar{v} \times \bar{B})$ and $\bar{\bar{\psi}}$ is called the kinetic stress tensor and is defined as

$$\bar{\bar{\psi}} = m\int_{-\infty}^{\infty}\!\!\int\!\!\int (\bar{w} - \bar{v})(\bar{w} - \bar{v})\ f\ d^3\bar{w} \quad . \qquad (2.9)$$

The continuity equation is an equation for the number density, n. It is not self-sufficient, however, because it introduces a new variable, the average velocity. The average velocity may be determined by solving the equation of momentum transfer if the stress tensor is known. The stress tensor is the solution of the third moment equation which is called the heat transport equation. There is an infinite number of moment

equations and each one introduces a new variable which couples that equation to the next higher moment equation. In order to obtain a finite set of equations in as many unknown variables, it is necessary to truncate the moment expansion by making a simplifying hypothesis about one of the macroscopic variables. In investigations of small amplitude waves in plasmas the moment equations are commonly truncated by making an assumption about the stress tensor, $\overline{\overline{\psi}}$. In fact, the two prevalent plasma models, the cold plasma model and the warm plasma model, are the result of two different assumptions for $\overline{\overline{\psi}}$. As has been mentioned, each of these models may be used to study wave propagation in a plasma and each model leads to different dispersion relations. These two models and their results will be discussed in greater detail.

The Cold Plasma Model

The most elementary assumption regarding the stress tensor is to assume that it is zero. This means that all thermal motion of the electrons is neglected or that the kinetic temperature of the electron gas is equal to zero. In this case the equation of momentum transfer becomes

$$nm \frac{d\overline{v}}{dt} = qn \overline{E} \tag{2.10}$$

in the absence of a magnetic field. If an $\exp(i\omega t)$ time dependence is assumed this equation may be solved for the velocity, $\overline{v}$, which may be used to calculate the current density as

$$\bar{J} = nq\bar{v} = \frac{q^2 n}{i\omega m}\ \bar{E} \tag{2.11}$$

One of Maxwell's equations is

$$\nabla_r x\ \bar{H} = \bar{J} + i\omega\varepsilon_o\ \bar{E} \tag{2.12}$$

Substituting the expression for current density one obtains

$$\nabla_r x\ \bar{H} = i\omega\varepsilon_o\ (1 - \frac{\omega_p^2}{\omega^2})\ \bar{E} = i\omega\varepsilon_o\varepsilon_p\ \bar{E} \tag{2.13}$$

where

$$\varepsilon_p \equiv 1 - \frac{\omega_p^2}{\omega^2} \tag{2.14}$$

is termed the relative dielectric constant for the plasma. Thus in the cold plasma model the plasma may be completely accounted for by considering it to be a dielectric with a frequency dependent dielectric constant.

The cold plasma model can be applied to the problem of wave propagation along a plasma column or a plasma slab. The surface wave modes are the only forms of propagating waves predicted by such an application of the cold plasma model. The surface wave modes are "slow waves", that is their phase velocity is less than the speed of light. For slow waves it can be shown that the electric field is given approximately as the gradient of a scalar potential, or

$$\bar{E} \simeq -\nabla_r\phi\ . \tag{2.15}$$

This approximation is termed the "quasi-static approximation". Under the quasi-static approximation the descriptive differential equation for wave propagation in a cold plasma can be obtained from

$$\nabla_r \cdot \varepsilon_p \overline{E} = 0 \tag{2.16}$$

which becomes

$$\nabla_r \cdot \varepsilon_p \nabla_r \phi = 0 \tag{2.17}$$

upon substitution of Eq. (2.15) for the electric field. By solving Eq. (2.17) for the potential, ϕ, and requiring that the potential meet the appropriate boundary conditions one obtains the cold plasma dispersion relation for the surface wave modes. If the plasma is homogeneous then ε_p is not a function of position and may be brought outside the divergence operation in Eq. (2.17). The equation becomes

$$(1 - \frac{\omega_p^2}{\omega^2})\nabla_r^2 \phi = 0. \tag{2.18}$$

The solution $\omega^2 = \omega_p^2$ represents the in-phase oscillation of the plasma at the plasma frequency and does not represent a wave-like solution. It is the solutions of

$$\nabla_r^2 \phi = 0 \tag{2.19}$$

that yield the surface wave modes. The results of a calculation of the dispersion relation for the cold plasma surface wave modes in a homogeneous plasma will be given later.

The Warm Plasma Model

The assumption that is made in the warm plasma model is that the divergence of the stress tensor may be replaced by the gradient of a scalar pressure in the equation of momentum transfer. Equation (2.8) becomes

$$nm \frac{d\bar{v}}{dt} = q\, n\, \bar{E} - \nabla_r p \tag{2.20}$$

for an isotropic plasma. In addition to the equation of momentum transfer, there are two other equations that are available in the calculation of the dispersion relation for the waves in a warm plasma. They are

$$\frac{\partial n}{\partial t} + \nabla_r \cdot (n\bar{v}) = 0 \tag{2.21}$$

and

$$\nabla_r^2 \phi = - \rho/\varepsilon_o \quad . \tag{2.22}$$

Equation (2.22) implies the quasi-static approximation. It is also assumed that the motion of the ions may be neglected. To solve this set of equations for the dispersion relation the equations must first be linearized. The electric field, the number density, the pressure, and the velocity are written as the sum of a steady state term (if one is present) and a time varying perturbation term which is due to the presence of the wave. These relations are

$$\bar{E} = - \nabla_r \phi_o - \nabla_r \phi_1 \, e^{i\omega t} \tag{2.23}$$

$$n = n_o(\bar{r}) + n_1(\bar{r}) e^{i\omega t} \tag{2.24}$$

$$p = p_o(\bar{r}) + p_1(\bar{r}) e^{i\omega t} \tag{2.25}$$

$$\bar{v} = \bar{v}_1 \, \varepsilon^{i\omega t} \tag{2.26}$$

These expressions are substituted into Eq. (2.20) through (2.22) and the products of perturbed terms are neglected. In the absence of a wave (the steady state situation) Eq. (2.20) yields the relationship between the steady state potential and pressure

$$q n_o \nabla_r \phi_o - \nabla_r p_o = 0 \tag{2.27}$$

In the presence of a wave these three equations yield

$$i\omega n_1 + \nabla_r \cdot (n_o \bar{v}_1) = 0 \tag{2.28}$$

$$i\omega n_o m \bar{v}_1 = q n_1 \nabla_r \phi_o + q n_o \nabla_r \phi_1 - \nabla_r p_1 \tag{2.29}$$

$$\nabla_r^2 \phi_1 = q n_1 / \varepsilon_o \quad . \tag{2.30}$$

By including equations of state that relate the pressures to the number densities, a set of equations is obtained which can be solved for the dispersion relation. In the steady state the electron gas is assumed to obey the ideal gas law, so

$$p_o = n_o k_B T \tag{2.31}$$

where k_B is Boltzmann's constant and T is the electron temperature. The perturbed pressure is assumed to be related to the perturbed number density by

$$p_1 = \gamma' n_1 k_B T \tag{2.32}$$

where the constant, γ', can be shown to be 3 [Delcroix, 1965] for linear adiabatic compression in a collisionless plasma. With these assumptions Eq. (2.27) through (2.30) can be rewritten as

$$q n_o \nabla_r \phi_o - k_B T \nabla_r n_o = 0 \tag{2.33}$$

$$i\omega n_1 + \nabla_r (n_o \bar{v}_1) = 0 \tag{2.34}$$

$$i\omega n_o m \bar{v}_1 = q n_1 \nabla_r \phi_o + q n_o \nabla_r \phi_1 - \gamma' k_B T \nabla_r n_1 \tag{2.35}$$

$$\nabla_r^2 \phi_1 = q n_1 / \varepsilon_o \quad . \tag{2.36}$$

Equations (2.33) through (2.36) may be combined to yield

$$\nabla_r^2 (\nabla_r^2 \phi_1) + k^2 \nabla_r^2 \phi_1 =$$

$$= \frac{\nabla_r \phi_1 \cdot \nabla_r \omega_p^2}{C_s^2} r \frac{1}{\gamma'} \left[\frac{1}{n_o} \nabla_r^2 \phi_1 \nabla_r^2 n_o - \frac{\nabla_r^2 \phi_1 (\nabla_r n_o)^2}{n_o^2} + \nabla_r n_o \frac{\nabla_r (\nabla_p^2 \phi_1)}{n_o} \right] \tag{2.37}$$

where

$$k^2 = \frac{\omega^2 - \omega_p^2}{C_s^2} \tag{2.38}$$

and

$$C_s^2 = \frac{\gamma' k_B T}{m} \tag{2.39}$$

C_s is the speed of sound in the electron gas. Equation (2.37) can be solved for the wave potential ϕ_1, given the steady state electron density profile, $n_o(\bar{r})$. These solutions are usually obtained numerically for most profiles of interest and this is frequently a lengthy process.

It is of interest at this point to obtain a solution to Eq. (2.37) for a homogeneous plasma in a geometry similar to that which will be used for the numerical simulation. These results will be compared with those obtained from the computer simulation later. The geometry is shown in Fig. 2.1. The plasma slab is confined between y = -a and y = +a by dielectric walls. There are perfectly conducting boundaries at y = -b and y = +b. The system is infinite in the x- direction and the z- direction which is perpendicular to the page. For a homogeneous plasma Eq. (2.37) reduces to

$$\nabla_r^2(\nabla_r^2\phi_1) + k^2\nabla_r^2\phi_1 = 0 \quad . \tag{2.40}$$

It will be assumed that ϕ_1 has no dependence on the z coordinate and ϕ_1 can be written as

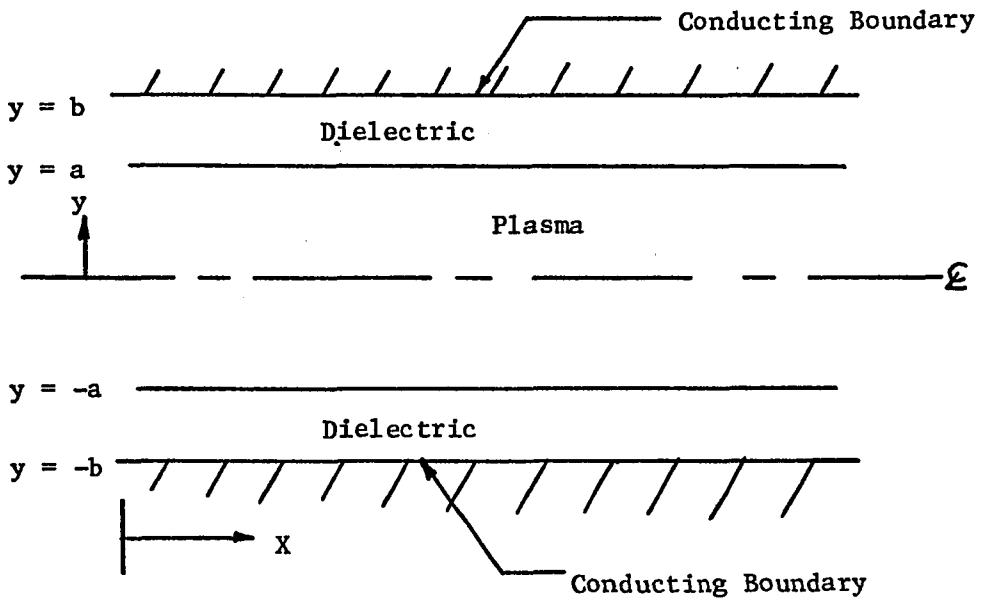

Fig. 2.1 Geometry for the Warm Plasma Model Solution

$$\phi_1 = \tilde{\phi}(y) \exp(-i\beta x) \quad .$$

Equation (2.40) becomes

$$\frac{d^4\tilde{\phi}}{dy^4} + (k^2-2\beta^2) \frac{d^2\tilde{\phi}}{dy^2} + \beta^2(\beta^2-k^2)\tilde{\phi} = 0 \tag{2.41}$$

the solution of which is

$$\tilde{\phi} = Ae^{\beta y} + Be^{-\beta y} + Ce^{i\gamma y} + De^{-i\gamma y} \tag{2.42}$$

where $\gamma^2 = k^2 - \beta^2$. In the dielectric regions the potential is a solution of Laplace's equation. The dispersion relation is obtained by applying the boundary conditions to the potential. The electrical boundary conditions are that the potential and the electrical displacement be continuous at the plasma-dielectric interface at $y = +a$ and $y = -a$. Also, the potential must be zero at the conducting boundaries at $y = +b$ and $y = -b$. The mechanical boundary condition is that the y-component of the velocity, $\bar{v}_1$, be zero at $y = +a$ and $y = -a$ since the dielectric is nonconducting and assumed to be rigid. To simultaneously satisfy these boundary conditions, one finds that the following determinant must be zero, or

$$\begin{bmatrix} e^{\beta a} & e^{-\beta a} & e^{i\gamma a} & e^{-i\gamma a} & -(e^{\beta a} - e^{\beta(2b-a)}) & 0 \\ e^{-\beta a} & e^{\beta a} & e^{i\gamma a} & e^{-i\gamma a} & 0 & -(e^{-\beta a} - e^{\beta(a-2b)}) \\ \beta e^{\beta a} & -\beta e^{-\beta a} & i\gamma e^{i\gamma a} & -i\gamma e^{-i\gamma a} & -\varepsilon_r \beta(e^{\beta a} + e^{\beta(2b-a)}) & 0 \\ \beta e^{-\beta a} & -\beta e^{\beta a} & i\gamma e^{-i\gamma a} & -i\gamma e^{i\gamma a} & 0 & \varepsilon_r \beta(e^{-\beta a} + e^{-\beta(2b-a)}) \\ se^{\beta a} & -se^{-\beta a} & ue^{i\gamma a} & -ue^{-i\gamma a} & 0 & 0 \\ se^{-\beta a} & -se^{\beta a} & ue^{-i\gamma a} & -ue^{i\gamma a} & 0 & 0 \end{bmatrix} = 0$$

(2.43)

where

$$s = -i\beta/\omega m \quad ,$$

$$u = \frac{\gamma}{\omega m}\left[1 + \gamma'\lambda_D^2\,(\gamma^2 + \beta^2)\right] \quad ,$$

and ε_r is the relative permittivity of the dielectric. λ_D is the Debye length and is given by

$$\lambda_D = \left[\frac{\varepsilon_o k_B T}{n_o q^2}\right]^{1/2} \quad .$$

ω versus β data may be obtained from Eq. (2.43) by numerical methods. Such an ω - β diagram for the warm plasma waves is shown in Fig. 2.2 along with the cold plasma model ω - β diagram. In this figure the frequency, ω, has been normalized to the plasma frequency, ω_p, and the propagation constant, β, has been normalized to the separation between the conducting planes, d. The dashed line marked C_s is the locus of points with the speed of sound, C_s, as their phase velocity, ω/β. In the cold plasma case the phase velocity of the surface wave modes tends to zero as ω approaches $\omega_p/(1 + \varepsilon_r)^{1/2}$. Whereas in the warm plasma model the phase velocity of the surface wave modes approaches the speed of sound, C_s, as β increases. The high pass modes which exist above the plasma frequency are called the Dattner modes. These modes are thermal in nature and are not predicted by the cold plasma model.

The warm plasma model is superior to the cold plasma model in that it does predict the additional modes, the Dattner modes, which

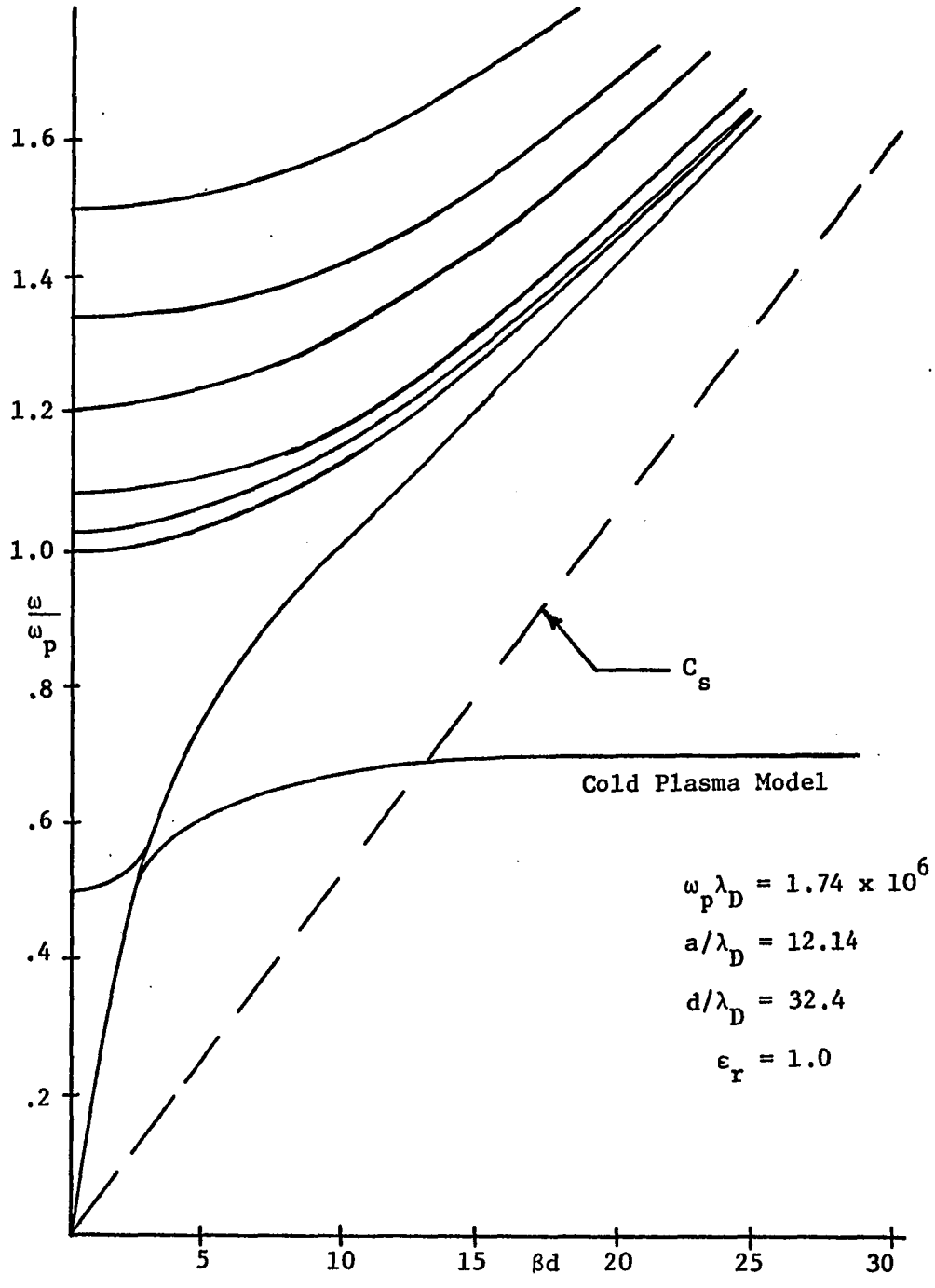

Fig. 2.2 ω-β Diagram of the Warm Plasma Model Contrasted with that of the Cold Plasma Model

propagate in the plasma system. The warm plasma model does have its disadvantages, however. The motion of the electrons is represented through an average velocity and the thermal spread in velocities as represented by the distribution function is not represented in the warm plasma model. Phenomena which are the result of the behavior of a fraction of the electron whose velocities differ from the average velocity do not appear in the warm plasma model. Landau damping is the most important example of this type of phenomena. Another limitation is placed on the warm plasma model by linearizing the equations. This means that only small amplitude waves may be studied. All nonlinear phenomena such as parametric interactions cannot be investigated with the warm plasma model. An example of a large amplitude wave application is the electromagnetic heating of a plasma.

The Computer Simulation Model

The computer simulation model overcomes the shortcomings ascribed to the warm plasma model. The computer simulation model is really a many body approach to the problem. Although it is impossible to follow the motion of all of the electrons in a laboratory plasma, it is possible to follow the motion of a small fraction of the electrons in the plasma with the aid of a digital computer. The number of electrons that can be followed is limited by the memory size and the speed of the digital computer. These few electrons represent a statistical sampling of the electrons in the laboratory plasma. The more electrons that are used in the computer simulation, the larger the statistical sample, and therefore the more accurate the resemblance of

the sample to the laboratory plasma. By following the motion of the sample electrons in time, the time evolution of the sample system may be observed. The evolution in time of the laboratory plasma may be inferred from this if the sampling is large enough. In this way the behavior of the laboratory plasma is simulated on a digital computer.

To make the computer simulation of a plasma practical certain numerical techniques must be employed and several restrictions must be placed on the type of system which can be simulated. These restrictions and techniques will be discussed in Chapter 3.

CHAPTER 3

COMPUTER SIMULATION OF A PLASMA

Finite Differences

The concept of a model for a system implies that certain approximations and assumptions are made with regard to the system to obtain a conceptual picture (or model) of the system which enables one to obtain solutions to problems concerning the system. The major limitations on a computer model of a plasma are those imposed by the digital computer itself. In the computer simulation of a plasma the motion of several thousand sample electrons is followed in time with the digital computer. The simulation proceeds stepwise in time as follows:

1. At the beginning of each time-step the charge density is computed from the stored positions of each particle.
2. The electric potential is calculated from the charge density using Poisson's equation. The electric field is then calculated from the electric potential.
3. The electric field is allowed to accelerate each particle individually over a short time step. The new positions and velocities for each particle are recorded and the cycle repeats at Step 1.

To obtain a meaningful simulation several thousand particles must be followed for a thousand or more time steps. On present day

digital computers only one and two dimensional problems may be simulated. In a two dimensional problem only four numbers are required to specify the state of a particle. In essence then one is watching the time behavior of charged rods. The limitation to two dimensional problems is due to the central memory size of digital computers. The numbers that specify the position and velocity of each particle as well as those that describe the potential distribution in the system must be stored within the central memory of the computer if one is to have an economical simulation. The alternate method would be to segment the data and store the segments on disk or tape files, then each segment could be read in from the file and worked on separately. However, this shuffling of information on to and off of files is time consuming and therefore expensive. In order to have an economic simulation, one must formulate the computer program such that each time step requires but a few seconds of computer time.

Two dimensional simulations are conveniently done in a rectangular coordinate system with rectangular boundaries. Consider the system shown in Fig. 3.1. The particles are free to move in the region $0 \leq x \leq L$ and $0 \leq y \leq W$. In this region the potential and the charge density are continuous functions of x and y. These continuous functions must be digitalized for use on a digital computer. This can be accomplished through the use of finite difference methods. Instead of allowing the x and y coordinates to be continuous, they are divided into increments of equal length. The x - axis is divided into M increments of length Δx each. The y - axis is broken into N increments of length

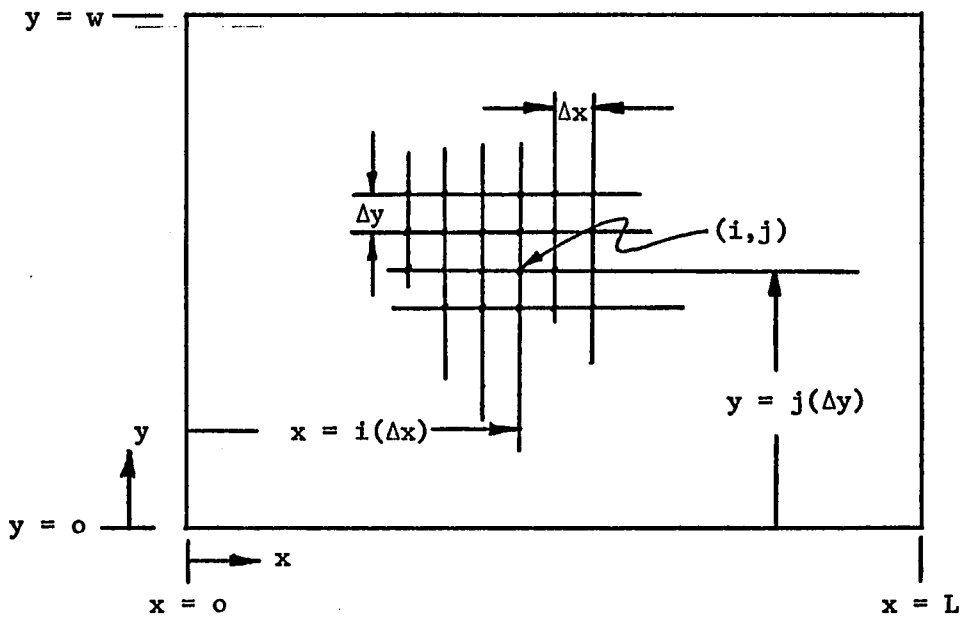

Fig. 3.1 Geometry for a Typical Two Dimensional Simulation System

Δy. Instead of stating the charge density and electric potential as a function of x and y, their spatial variation is described by giving its value at the various mesh points. The x coordinate of a mesh point can be specified by an integer, i, as

$$x = i(\Delta x) \quad ,$$

$$i = 0, 1, \ldots M. \tag{3.1}$$

Similarly, the y coordinate of a mesh point can be specified by an integer, j, as

$$y = j(\Delta y) \quad ,$$

$$j = 0, 1, \ldots N. \tag{3.2}$$

The charge density and electric potential at the mesh point (i,j) are denoted $\rho_{i,j}$ and $\phi_{i,j}$, respectively. Thus, the electric potential and charge density functions are replaced by two dimensional arrays.

The substitution of an array for the electric potential function necessitates the replacement of the various derivatives of the electric potential by appropriate differences of the potential array, $\phi_{i,j}$. The partial derivatives of ϕ with respect to x and y are replaced by the first difference of $\phi_{i,j}$ in x and y.

$$\left.\frac{\partial \phi}{\partial x}\right|_{x=i(\Delta x)}$$

is replaced by

$$\Delta_x \phi_{i,j} = \frac{\phi_{i+1,j} - \phi_{i,j}}{\Delta_x} \tag{3.3}$$

and

$$\left.\frac{\partial \phi}{\partial y}\right|_{y=j(\Delta x)}$$

is replaced by

$$\Delta_y \phi_{i,j} = \frac{\phi_{i,j+1} - \phi_{i,j}}{\Delta_y} \tag{3.4}$$

Note that in the limit as Δx or Δy approach zero, these differences become the definitions of the partial derivatives. Poisson's equation involves the second partial derivatives of the electric potential with respect to x and y. The second partial of ϕ with respect to x is approximated by

$$\frac{\Delta_x \phi_{i,j} - \Delta_x \phi_{i-1,j}}{\Delta_x}$$

$$= \frac{\phi_{i+1,j} + \phi_{i-1,j} - 2\phi_{i,j}}{(\Delta x)^2} \tag{3.5}$$

and the second partial of ϕ with respect to y is approximated by

$$\frac{\Delta_y\phi_{i,j} - \Delta_y\phi_{i,j-1}}{\Delta_y}$$

$$= \frac{\phi_{i,j+1} + \phi_{i,j-1} - 2\phi_{i,j}}{(\Delta_y)^2} \tag{3.6}$$

Poisson's equation in two dimensions is

$$\frac{\partial^2\phi}{\partial x^2} + \frac{\partial^2\phi}{\partial y^2} = -\rho/\varepsilon_o \tag{3.7}$$

Using the approximations in Eq. (3.5) and (3.6) this becomes

$$\frac{\phi_{i+1,j} + \phi_{i-1,j} - 2\phi_{i,j}}{(\Delta_x)^2} + \frac{\phi_{i,j+1} + \phi_{i,j-1} - 2\phi_{i,j}}{(\Delta_y)^2} = -\rho_{i,j}/\varepsilon_o \tag{3.8}$$

in finite difference form. Equation (3.8) relates the electric potential at the mesh point (i,j) to the charge density at this mesh point and the electric potential at the adjacent mesh points above and below, and to the right and left of it. An equation such as Eq. (3.8) may be written for every mesh point within the system, then with appropriate boundary conditions on the electric potential one has a system of simultaneous equations to be solved for the electric potential at the mesh points.

The Calculation of Charge Density

In a computer simulation of plasma there are typically several thousand sample particles used to represent the behavior of the 10^{10} particles in the real plasma. Therefore each sample particle followed

by the computer represents about 10^6 electrons. At the beginning of a computer simulation each sample particle is assigned a location in phase space; that is, it is given an initial position in the system and an initial velocity. For example, the particles might be initially distributed uniformly throughout the system and given a Maxwellian velocity distribution. In the phase space of the real plasma system, there are 10^{10} points each of which represents the state of an electron in the plasma. If one subdivides this phase space into cells such that each cell contains an equal number of points, say 10^6 points, one would have 10^4 cells, each containing electrons whose initial velocities and initial positions are very nearly equal. By selecting one arbitrary electron from each cell one obtains a statistical sample of the electron in the plasma. The motion of these sample electrons may be followed by means of a digital computer and each "computer electron" represents the 10^6 electrons in the real system which had their initial positions and velocities very nearly equal to each other and to sample electron which is followed on the computer. This fact is important in the computation of the charge density at the beginning of each time step. The charge that a single rod contributes to a grid point in the computation of the charge density is not merely the electronic charge of a single electron but typically 10^6 times the charge of a single electron since each rod represents about 10^6 electrons in the real plasma. This must be done so that the potential and electric field calculated in the computer simulation will be the same as that in the laboratory plasma.

From the known position of each of the rods, one must compute the charge density at each mesh point. Perhaps the simplest way to do this would be to assign all the charge associated with a given rod to the nearest grid point. In Fig. 3.2 the location of the electron is marked by an "x". The grid point nearest the electron is the (i,j) mesh point and so all the charge associated with this electron rod would be assigned to the mesh point (i,j). There is a serious disadvantage to this technique however. During some time step the electron rod will go from the vicinity of one mesh point to the vicinity of a neighboring mesh point. During this step the charge associated with the first grid point decreases abruptly while the charge associated with the second grid point increases abruptly. This causes erratic fluctuations in the resultant electric potential. A simple way of improving this situation has been suggested by Birdsall and Fuss [1969]. In this method the charge associated with a rod is assumed to be uniformly distributed throughout a rectangular cross section of dimensions Δx by Δy as is shown in Fig. 3.2. The charge due to a given electron is then shared among the four grid points nearest the rod. The portion of the charge which is assigned to each of the nearest grid points is proportional to the amount of area of the rod that lies within the cell associated with each grid point as indicated in Fig. 3.2 Therefore, if the nearest grid point to the rod is the grid point (i,j), the charge of that rod is shared between grid points (i,j), (i-1,j), (i,j-1), and (i-1,j-1) for the configuration shown in Fig. 3.2. As a particle moves in time its charge gradually shifts from one grid point to a neighboring grid

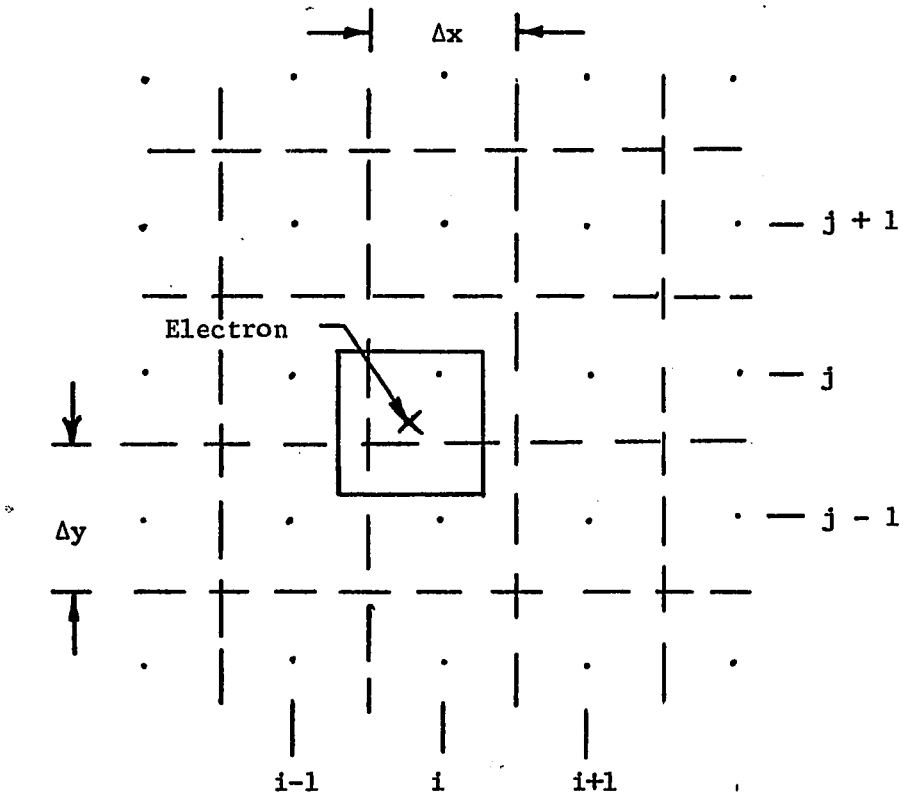

Fig. 3.2 Illustration of Charge Sharing Among the Four Grid Points Nearest the Electron

point. This eliminates the abrupt changes in the charge density on the grid points. This approach is called the "Cloud-in-Cell" method by Birdsall and Fuss [1969].

A third approach to plasma simulation is due to Kruer and Dawson [1969]. In this method the total charge associated with a rod is also distributed over an extended area. However, the distribution of the charge over the area is Gaussian rather than uniform as it is in the "Cloud-in-Cell" method. The approach of Kruer and Dawson differs from the "Cloud-in-Cell" method in a second, important aspect also. The "Cloud-in-Cell" method calculates the electric field from the charge density at each grid point, whereas Kruer and Dawson not only utilize the charge density but also the dipole moment of the charge density at each grid point in computing the electric field. This results in a more accurate value for the electric field and therefore less numerical error in the plasma simulation. The major disadvantage of this method is that it requires three times as much computer central memory as does the "Cloud-in-Cell" method. This limits the application of the technique to those computers with very large central memories. For this reason the "Cloud-in-Cell" method was used exclusively in the computer simulation experiments to be described later.

Particle Acceleration

The x and y components of the electric field may be computed from the electric potential. The components of the electric field at grid point (i,j) are given by

$$E_x = \frac{\phi_{i-1,j} - \phi_{i+1,j}}{2(\Delta_x)} \tag{3.9}$$

and

$$E_y = \frac{\phi_{i,j-1} - \phi_{i,j+1}}{2(\Delta_y)} \tag{3.10}$$

An electron rod is accelerated by the electric field at grid point nearest the rod. This is termed the nearest grid point approximation. Since the electron rods are not accelerated by the electric field at the exact location of the rod itself, an error in the trajectory of the rod may result if the electric field at the nearest grid point is very different from that which would exist at the electron rod. This error may be greatly reduced if the mesh spacing is chosen such that the electric field does not vary greatly from a grid point to its neighbor. A measure of the shortest distance over which collective phenomena can vary in a plasma is the Debye length. Therefore, a first criterion for a successful simulation is that the mesh size be less than or equal to the Debye length.

Using the electric field at the nearest grid point the velocity of an electron is incremented by an amount $\Delta\bar{v}$ given by

$$\Delta\bar{v} = -\frac{q}{m}(\Delta t)\bar{E} \tag{3.11}$$

where q is the electronic charge, m is the electronic mass, Δt is the length of a time step, and $\bar{E}$ is the electric field at the nearest grid

point. Using the new velocity the position of an electron is increment an amount $\Delta\bar{r}$ given by

$$\Delta\bar{r} = \bar{v}(\Delta t) \tag{3.12}$$

where $\bar{v}$ is the new velocity of the electron.

Equations (3.11) and (3.12) are used to compute the position and velocity of each electron at a time step from those at the previous time step. While this is the actual computation process carried out by the computer, it is advantageous to view the procedure in a different manner. This viewpoint is termed "leap-frogging" and is described in detail in in the literature [Hockney, 1967; Buneman, 1967]. In "leap-frogging" one views the electric field and particle positions as being given on the integer time steps, and the particle velocities as being given at half integer time steps. This results in a time-centered integration of the particle trajectories. "Leap-frogging" is actually a conceptual change as far as computing particle trajectories is concerned. The only time that "leap-frogging" alters the actual calculation is if one wishes to compute the positions and velocities of the particles at the same instant of simulation time as, for example, one would in computing the total energy of the system. In computing the total system energy one cannot simply use the positions (or electric fields) and the velocities that are currently in the memory of the computer since they are values possessed by the system at two different times separated by one half a time step. To compute the total energy one must compute the velocities that the electrons possessed a half time step prior to the values

currently stored in the computer memory. The "leap-frogging" philosophy was used throughout the computer experiments described in this work.

The electron plasma frequency, ω_p, is the natural frequency of oscillation of the electron gas. In order for the computer simulation to be numerically stable the time increment must be chosen so that it is smaller than a period of the plasma frequency or

$$\Delta t << \frac{2\pi}{\omega_p} \quad . \tag{3.13}$$

Equation (3.13) is a second criterion for a successful plasma simulation.

The Size of the Statistical Sample

Not all collections of mobile ions and electrons exhibit plasma-like behavior. The most marked characteristic of a plasma is the tendency of the charged particles to oscillate at their plasma frequencies. In order for the electron gas to exhibit collective behavior such as plasma oscillation, it is necessary for the electron collision frequency, ν, to be much less than the electron plasma frequency. It can be shown that the ratio ν/ω_p will be small if the number of electrons, in a spherical volume whose radius is a Debye length, is very large [Kunkel, 1966]. If the number of electrons in a Debye sphere is large, the collision frequency will be much less than the plasma frequency and the electron gas will exhibit collective behavior.

There is an analogous restriction that must be placed on a computer simulation plasma if it is to behave like a real plasma and exhibit collective behavior. In a two-dimensional simulation one requires

that there be several electron rods in a square whose side is a Debye length long. Typically one finds that the number of electron rods in a Debye square, N_D, must be at least five. This ensures that the collision frequency will be at least an order of magnitude less than the plasma frequency [Hockney, 1966; Okuda, 1969]. This, therefore, is a third criterion for a successful computer simulation of a plasma. The number of electron rods that must be followed by the digital computer depends on the dimensions of the system one is simulating in units of the Debye length.

Dawson [1962, 1964] has studied the statistical properties of simulation systems composed of from nine to several thousand electrons. The thermalizing properties and ergodic behavior of the systems were investigated and found to be in agreement with the assumption that one is equally likely to find the system in equal volumes of available phase space. The velocity distribution, drag on fast particles, Landau damping of Fourier modes, as well as other properties were found to be in agreement with theoretical values.

CHAPTER 4

THE COMPUTER EXPERIMENT

Computer Simulation System Geometry

The computer simulation experiment was performed using the geometry shown in Fig. 4.1. The z-axis is perpendicular to the page. The conducting planes and the dielectric layers extend infinitely in the positive and negative z direction. Electron rods are free to move in the region between the dielectric layers. When an electron rod reaches one of the layers, it is specularly reflected. This boundary condition is chosen in this manner to resemble what happens to an electron in a real plasma discharge. In a laboratory plasma a negative surface charge of electrons forms on the dielectric boundary resulting in an inhomogeneous plasma and a plasma sheath at the plasma-dielectric boundary. This sheath forms when the discharge is initiated and serves to prevent additional electrons from actually reaching the dielectric boundary. An electron nearing the wall is repelled by the negative surface charge on the wall and the net result is that the electron is reflected back into the plasma as if it had suffered a specular reflection with a rigid body. Only those few electron with sufficient kinetic energy to overcome the potential barrier between the dielectric wall and the body of the plasma actually reach the wall.

The system is assumed to be periodic in the length L in the x direction. If an electron leaves the system at x=L, it re-enters the

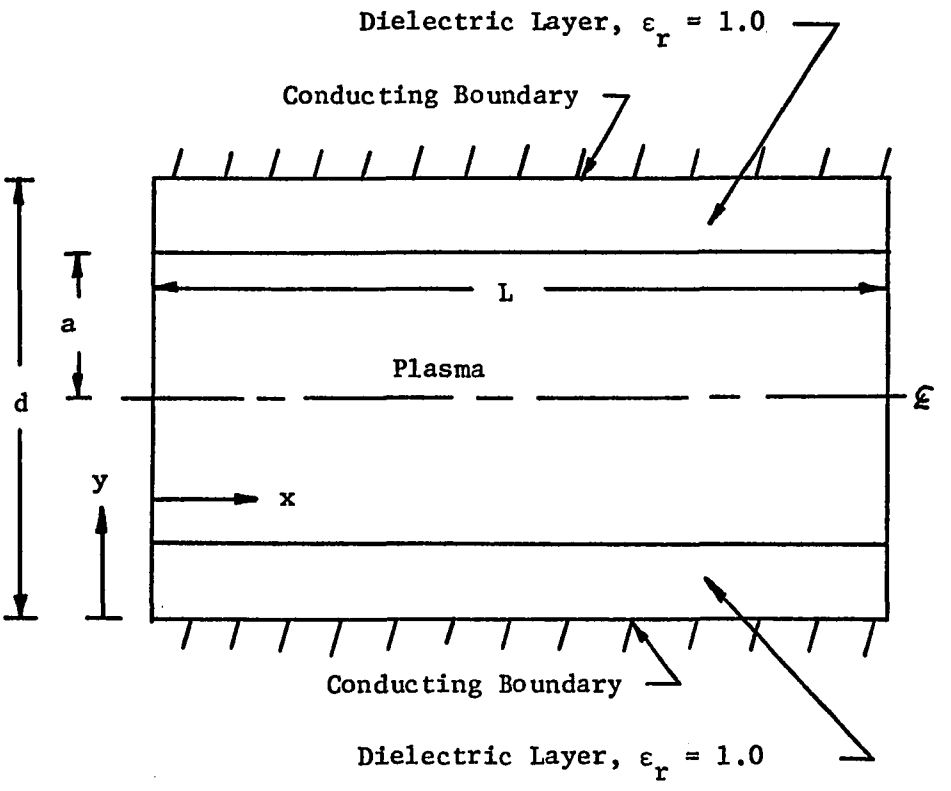

Fig. 4.1 Computer Simulation Geometry

system at x=0 with its y coordinate and its velocity unchanged. Similarly, if an electron leaves the system at x=0, it re-enters the system at x-L, again with its y coordinate and velocity unchanged.

The system shown in Fig. 4.1 will support wave modes which are symmetric and those which are asymmetric about the centerline at y=d/2. A great savings in computer time and therefore expense can be achieved by studying only those modes which are symmetric about the centerline. If the modes are purely symmetric, then one only need follow the motion of the electrons in the lower half of the system since the motion of the electrons in the upper half of the system is a mirror image of those below the centerline. This reduces the size of the statistical sample by half and means the computer need only perform half as many calculations of velocity and position changes for the symmetric mode case. This simplification and savings of computer time is applicable to the symmetric modes only. Also, the charge density need only be calculated in the lower half of the system since the values obtained in the lower half of the system may be reflected about the centerline to give the values in the upper half of the system. If the electron rods are to be restricted to the lower half of the simulation system, a boundary condition must be provided for an electron rod which reaches the centerline of the system. For symmetric modes every electron in the lower half of the system has a counterpart electron in the upper half of the system whose motion is the mirror image of the electron in the lower part of the system. If an electron crosses the centerline from the lower half of the system to the upper half, its counterpart electron

must simultaneously cross the centerline of the system at the same point with the same x-component of velocity. The net result is as if the original electron was specularly reflected by the centerline. More exactly, when an electron rod reaches the centerline, it trades identity with its counterpart electron from the upper half of the system.

The purpose of this work is to demonstrate the applicability of a computer simulation model for a plasma. The computer simulation results reported in this work are limited to the symmetric modes because of the economic advantages inherent in studying these modes.

The Computer Simulation Program

At the beginning of a computer simulation run each electron rod is assigned an initial position and an initial velocity. The initial velocities are assigned to give a Maxwellian velocity distribution corresponding to an electron temeprature, T. The electron rods are initially distributed uniformly in the x-direction. The electron rods may be given any distribution in the y-direction which has a zero slope at the centerline of the system. The distribution chosen for the initial demonstration of the computer simulation model was uniform in the y-direction. The results from this simulation may then be compared with the results that were obtained using the warm plasma model in Chapter 3.

The ions in the computer simulation are immobile. The ion density at each grid point is computed at the beginning of a computer run and remains constant throughout the simulation run. If the initial

electron density distribution is inhomogeneous in the y-direction, the initial ion density at each grid point may be determined from the electron density at the grid point and Eq. (2.22) and (2.33). When the initial electron density is uniform in the y-direction, the ion charge density is chosen to be the negative of the initial electron charge density at each grid point. For the uniform initial distribution case the system is exactly space charge neutral at the beginning of the first time step. The entire energy of the system is the kinetic energy of the electrons at the initiation of a simulation run.

The electron charge density is computed from the positions of the electrons using the charge sharing scheme described in Chapter 3. The total charge density is obtained by adding the constant ion charge density to the electron charge density at every grid point. The electric potential is calculated from the charge density using the Poisson solver program POT1 developed by Hockney [1968]. This computer subroutine was modified by the author so that its statements would be in proper FORTRAN IV syntax. This subroutine calculates the electric potential from the charge density subject to boundary conditions at x=0 and x=L, and y=0 and y=d. The subroutine allows three different boundary conditions. For example, the three boundary conditions as applied to the x-direction are as follows:

1. The potential may be specified at x=0 and x=L.
2. The normal derivative of the potential may be specified at x=0 and x=L.

3. The potential may be specified to be periodic in the length, L. The potential at x=0 is the same as the potential at x=L and the potential at $x=X_o$ is the same as the potential at $x=X_o+L$.

The same three choices of boundary conditions apply in the y-direction. One may mix the types of boundary condition using one in the x-direction and another in the y-direction. This was done in the computer simulation model for a bounded plasma. There are perfectly conducting planes at y=0 and y=d and so the potential is specified to be zero along these boundaries in the computer program. Since the system has been assumed to be periodic in the x-direction, the potential is also specified to be periodic in the length L in the computer program. The subroutine POT1 requires that the number of mesh points in the x and the y direction be some integer power of two. The mesh sizes, Δx and Δy need not be equal, however. The computer simulation model has 64 mesh spaces in both the x and y direction. $\Delta x/\lambda_D = 0.500$ and $\Delta y/\lambda_D = 0.505$ in the computer model.

Every five time steps the program prints out sample data. At the same time the program writes the potential on every grid point onto a magnetic tape for later analysis. The most important part of the sample data which is printed out every five time steps is the system energy. The computer program computes and writes out the kinetic energy, the potential energy, and the total energy of the system. Since there are no external forces acting on the plasma the total energy of the

system should ideally be conserved. However, because of the numerical approximations used and computer rounding error involved in the numerous arithmetic operations every time step, the total energy of the system is not conserved exactly. Typically, the total energy of a simulation plasma will rise slowly during the course of the computer simulation. A measure of the accuracy of a plasma simulation program is the net rise in total energy expressed as a percentage of the initial total energy of the system. The percentage increase in total energy may be reduced by increasing N_D, the number of electron rods in a Debye square and by decreasing Δt, the length of the time interval per step. In the computer simulation experiments performed there were 12.9 electron rods per Debye square and the time interval was 1/30 of a plasma period, $2\pi/\omega_p$. The simulation was carried out for 1500 time steps or 50 plasma periods. The increase in total energy was 8% or an average increase of 0.005% per time step. Figure 4.2 shows the total system energy and the potential energy plotted versus time during the symmetric wave simulation. Energy is plotted on a relative magnitude scale and the time is measured in terms of plasma periods. The graph of kinetic energy is omitted for clarity since it would be virtually indistinguishable from the total energy graph. Figure 4.3 is a depiction of the dependence of the percent increase in total energy on the number of electron rods in a Debye square, N_D. The simulation code was run for 200 time steps in each case. A different value of N_D was used for each run and the percent increase in total energy computed on the basis of 200 time steps. It is apparent that energy conservation

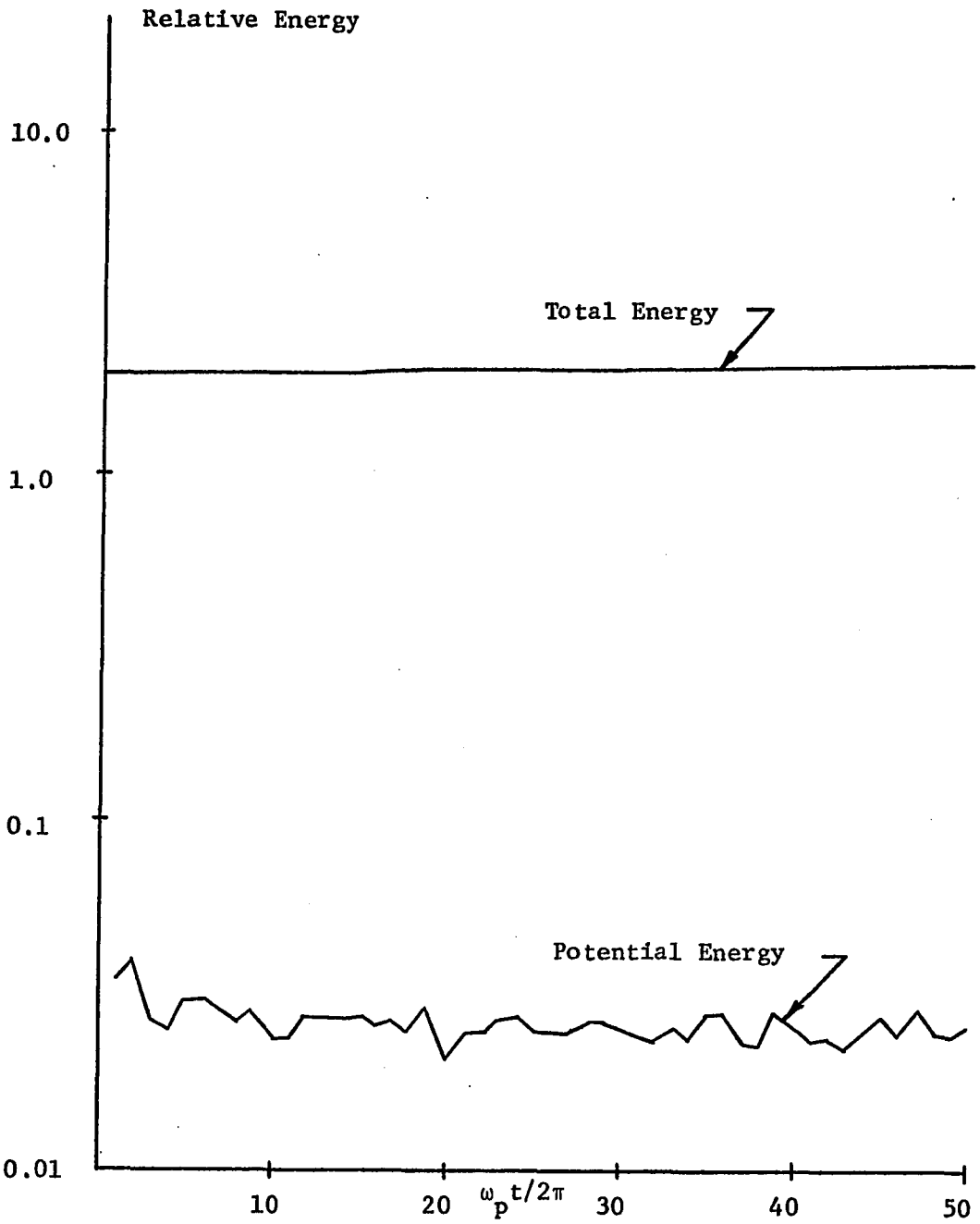

Fig. 4.2 Total System Energy and Potential Energy Versus Time Measured in Plasma Periods

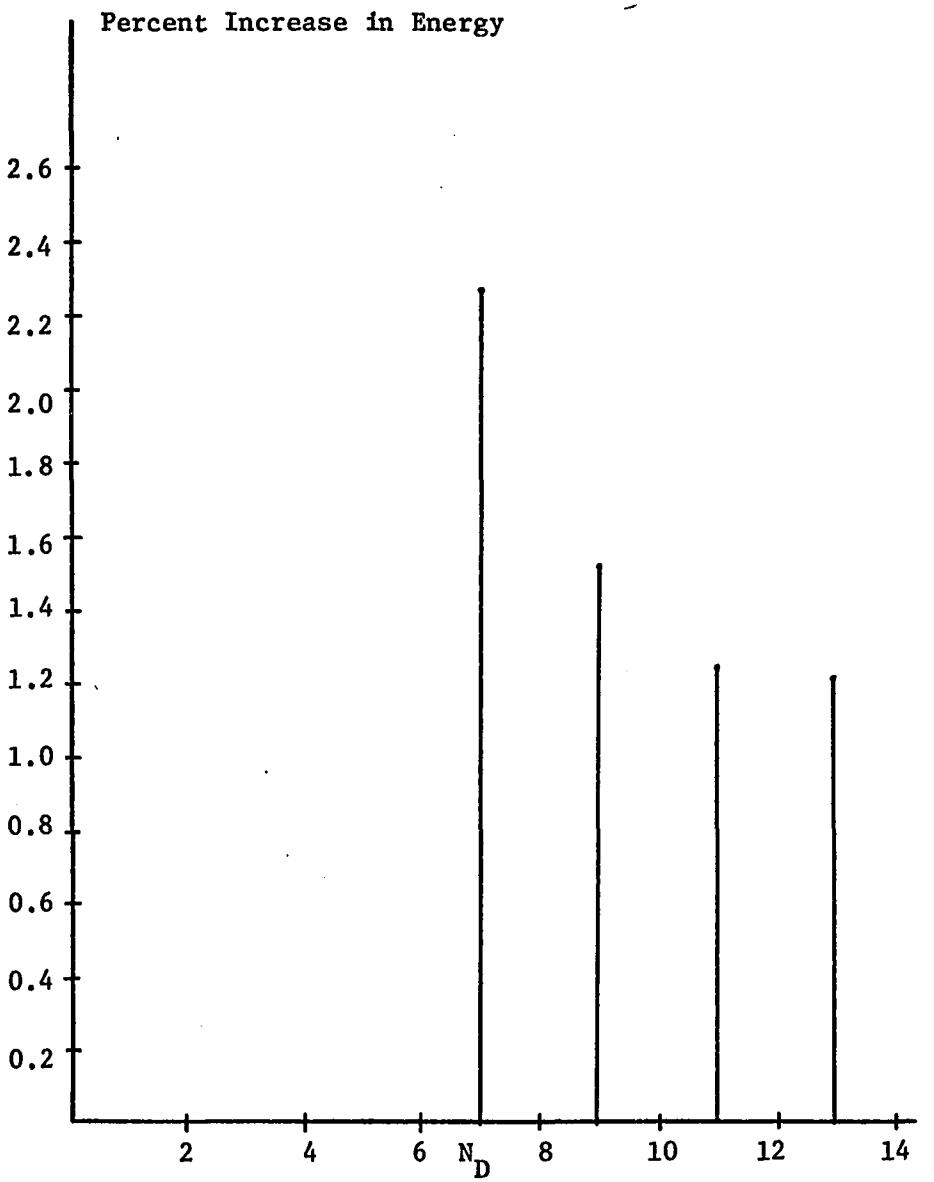

Fig. 4.3 Percent Increase in Total System Energy as a Function of N_D

improves as N_D increases. The upper limit on N_D is imposed by the size of the system in terms of Debye lengths and by the number of electron rods whose coordinates may be stored within the central memory of the computer. The plasma simulation experiments described in this work were performed on The University of Arizona's CDC 6400 digital computer. The central memory size of this computer limited the maximum number of electron rods to 5000.

Data Analysis

Every five time steps the potential on every grid point is written onto a magnetic tape for later analysis. At the completion of the computer simulation a complete record of the time dependent behavior of the potential at every grid point in the system is available on the magnetic tape. This tape may be used as input data for a second program which investigates the spatial and temporal behavior of the potential for wave-like behavior. Waves are excited in the simulation system by those particles moving at velocities greater than the thermal velocity of the electron gas. These fast particles leave wakes behind them as they pass through the background plasma [Dawson, 1962, 1964, 1968]. The wakes excite the waves which propagate in the system. Energy is continually being put into the modes of the system by these wakes, thereby causing the amplitudes of these modes to grow. The modes lose energy due to Landau damping and to some extent due to collisional loss. The collision frequency in the computer experiments performed was $\nu = 0.008\ \omega_p$ [Okuda, 1969; Birdsall, 1970]. The amplitudes of the modes grow until the energy supplied to each mode by the

wakes is balanced by the energy lost by the mode due to Landau damping and collisions. A mode is strongly Landau damped as its phase velocity approaches the thermal velocity. The steady state amplitude of a mode in this region of the ω-β diagram will consequently be much smaller than the wave amplitudes in the region of higher phase velocity. In the computer experiments reported in this work, the wave amplitudes decreased with decreasing phase velocity as expected.

Since the potential is periodic in the x-direction in the length. L, it may be expressed as a Fourier series as

$$\phi(x,y,t) = \sum_{n=o}^{\infty} [C_n(y,t) \cos(\beta_n x) + C_n'(y,t) \sin(\beta_n x)] \tag{4.1}$$

where $\beta_n = 2\pi n/L$. Since only the potential on the grid points is of interest, the series may be rewritten as a finite series

$$\phi_{i,j}(t) = \sum_{n=o}^{32} [C_n(j,t) \cos(i\Delta x\beta_n) + C_n'(j,t) \sin(i\Delta x\beta_n)] \tag{4.2}$$

where the integer i is redefined to refer to the x coordinate, $x = i(\Delta x)$; and the integer j refers to the y coordinate, $y = j(\Delta y)$. There are 64 mesh spaces in both the x and the y direction so $\Delta x = L/64$ and $\Delta y = d/64$. The wavevector amplitudes C_n and C_n' for an arbitrary value of j (or y) may be determined by Fourier analyzing the potentials which are recorded on the magnetic tape. This may

be done at every time step. This enables one to obtain the time dependence of each wavevector. The temporal variation of a wave amplitude is the sum of two terms. The first term is periodic in time with an angular frequency, ω, and is due to the propagation of a wave. This first term is the signal term. The second term is random in time and is due to the presence of noise in the plasma simulation. The noise arises naturally during the simulation since the charge in the system is in discrete particles and since these particles have random thermal velocities. This results in the presence of shot and thermal noise in the computer simulation. Therefore, C_n and C_n' may be represented as the sum of a signal term with frequency, ω, and a noise term which is random. For example, consider $C_n(j,t)$. One may write it as

$$C_n(j,t) = \Phi_n(j) \sin(\omega t+\theta) + g_n(t) \tag{4.3}$$

where θ is the phase angle of the signal and the function $g_n(t)$ represents the random noise associated with the n^{th} wavevector. One must determine the angular frequency, ω, of the n^{th} wavevector in Eq. (4.3) to obtain a data point for an ω-β diagram of the modes which propagate in the plasma simulation system. This determination would be trivial if it were not for the presence of the random noise, $g_n(t)$. If there were no noise present, one could merely calculate the wavevector at each time step from the potentials stored on the magnetic tape. By inspection, one could determine the period associated with a given wavevector and thereby calculate the frequency. The presence of the

random noise, however, makes the determination of the period difficult. It is necessary to first reduce or eliminate the effect of the noise on the wavevector amplitudes. This may be accomplished by time correlation of the wavevector amplitudes. Define the autocorrelation function of a wavevector amplitude, C_n, as

$$R_n(j,\tau) \equiv \frac{1}{T}\int_o^T C_n(j,t) \cdot C_n(j,t+\tau)dt \quad . \tag{4.4}$$

This integration may be performed numerically from the data stored on the magnetic tape. Substituting (4.3) into (4.4) one obtains

$$R_n(j,\tau) = \frac{1}{T}\int_o^T \Phi_n^2(j)\ \sin(\omega t+\theta) \cdot \sin\ [\omega(t+\tau)\ +\theta]dt \ .$$

$$+ \frac{1}{T}\int_o^T \Phi_n(j)\ \sin(\omega t+\theta)\cdot g(t+\tau)dt$$

$$+ \frac{1}{T}\int_o^T \Phi_n(j)\ \sin[\omega(t+\tau)+\theta] \cdot g(t)dt$$

$$+ \frac{1}{T}\int_o^T g(t) \cdot g(t+\tau)dt \quad . \tag{4.5}$$

The middle two terms represent the correlation between the signal and the random noise. These two terms are neglected on the assumption that

the signal and the random noise are uncorrelated, and therefore if the time of correlation, T, is long enough, these two integrals will be zero. The first integral has the particularly simple result of

$$\frac{1}{2}\,\Phi_n^2(j)\,\cos(\omega\tau)$$

when the correlation time, T, is an integer number of periods of the frequency, ω. The last integral is the correlation of the random noise with itself. The correlation of the noise will be denoted by $r_n(j,\tau)$. Since the noise is a random function of time, its value at a time t should bear little relation to its value τ seconds later. The product of the noise term at a time t with the noise term τ seconds later is equally probable to be positive as negative. When one integrates this product over time, successive parts of the integral tend to subtract from each other causing the value of the integral to be small. This is in contrast with the integral of the signal term. The signal is periodic and so there is a relationship between the value of the signal at a time t and the value of the signal τ seconds later, for all τ. Therefore, one expects that autocorrelation will reduce the noise amplitude in relation to the signal amplitude and $r_n(j,\tau)$ will be small, thereby facilitating the determination of the frequency associated with a wavevector. The result of correlating the wavevector amplitude is

$$R_n(j,\tau) = \frac{1}{2}\,\Phi_n^2(j)\,\cos(\omega\tau) + r_n(j,\tau) \quad . \tag{4.6}$$

The frequency spectrum of $R_n(j,\tau)$ may be obtained by Fourier analyzing $R_n(j,\tau)$. If there is indeed a periodic signal present, the amplitude of frequency component ω should be much larger than the other frequency components which are the frequency components of $r_n(j,\tau)$. An example of this is shown in Fig. 4.4. This figure shows the frequency spectrum of the lowest order wavevector in the system. The wavevector amplitudes were obtained by Fourier analyzing the potential on the centerline (j=32) of the system. There is a sharp rise in the amplitude at a frequency of $\omega/\omega_p = 1.125$ indicating the presence of a wave in the system at this frequency. The other frequency amplitudes constitute the frequency spectrum of the correlated noise, $r_n(j,\tau)$. It can be seen that the noise spectrum is virtually independent of frequency, or white noise. From Fig. 4.4 one can determine that there is a wave with a normalized propagation constant of $\beta d = 6.357$. A similar analysis may be carried out on the lines of constant y in the system and each wavevector may be analyzed to determine the frequency of the wave propagating with that value of propagation constant. Once one has determined a value of frequency and propagation constant which corresponds to a propagating wave, one may plot that frequency amplitude for the corresponding wavevector as a function of y (or j) to observe the variation of the wave potential in the direction transverse to the direction of propagation. The results of these studies are presented in the next section.

Computer Simulation Results

Figure 4.5 shows the ω-β data obtained from the symmetric wave simulation. The solid curves are the warm plasma model curves for the

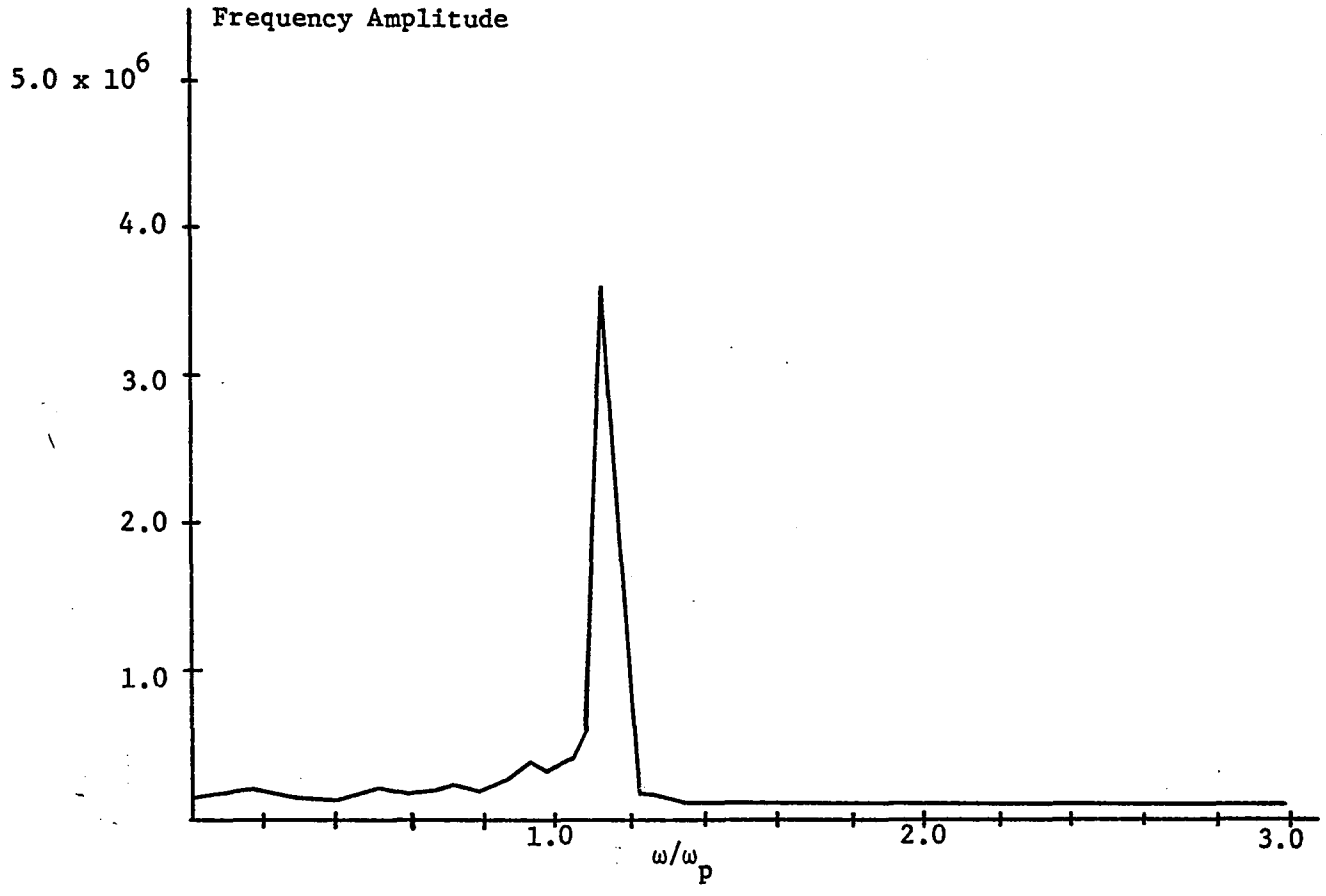

Fig. 4.4 Frequency Spectrum for the Lowest Order Wavevector on the Centerline (j = 32), βd = 6.357

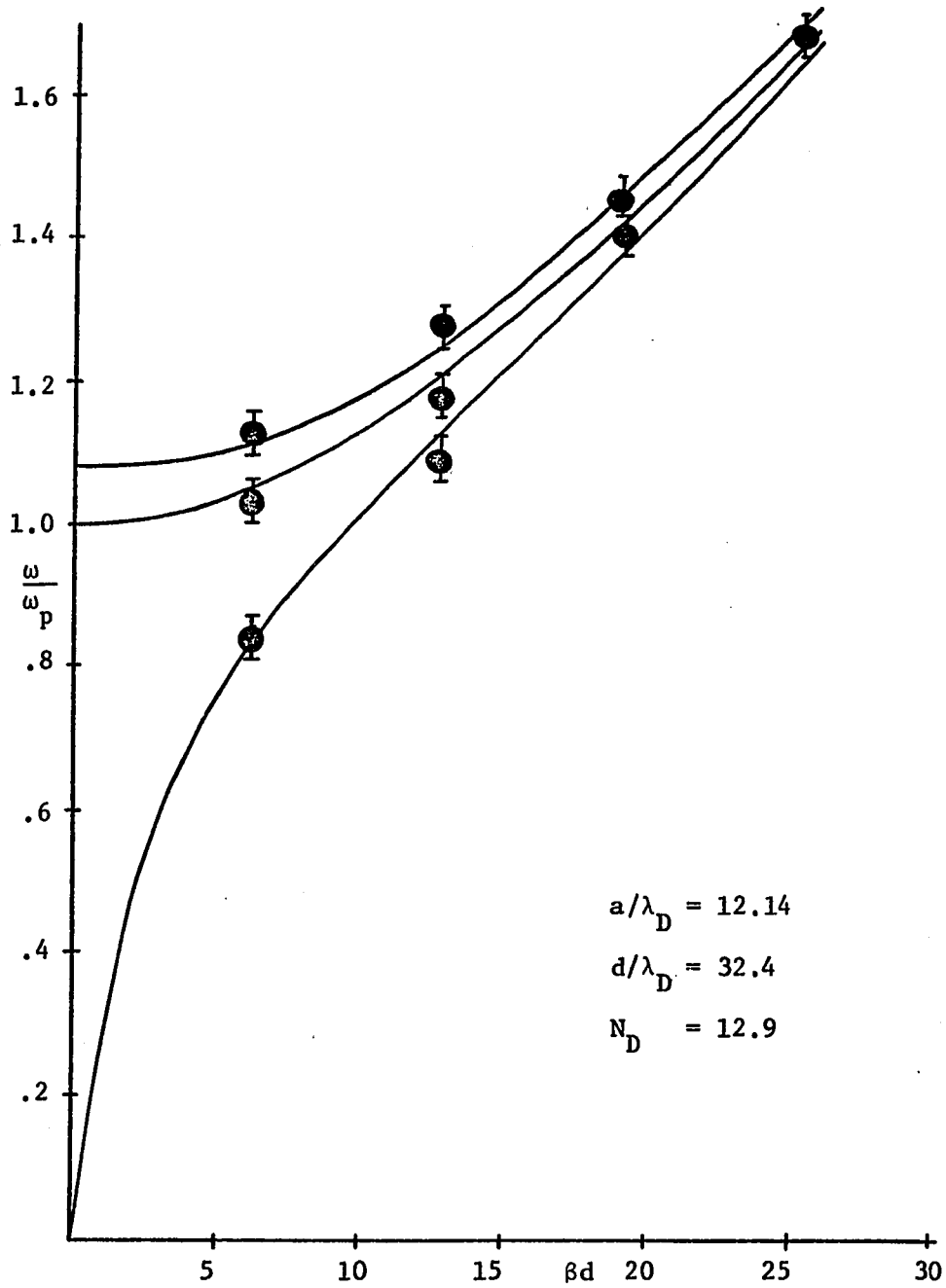

Fig. 4.5 ω-β Data from the Symmetric Wave Simulation

three lowest order symmetric modes presented in Chapter 2. The solid dots represent the data obtained from the plasma simulation program. The vertical line through each dot indicates the limit of frequency resolution in analyzing the plasma simulation data. This frequency resolution (or error) may be improved by increasing the length of the computer simulation run.

In Fig. 4.6(a) and Fig. 4.7 is shown the variation of the surface wave mode amplitude (squared) across the system for $\beta d = 6.357$ and $\beta d = 12.71$, respectively. There is good qualitative agreement with the predictions of the warm plasma model which are also shown. One can observe that as the propagation constant, β, increases, the energy in the surface wave modes becomes confined to the dielectric-plasma interface as is predicted by both the warm and cold plasma model. These simulation results dramatically illustrate the effect of the bounding dielectric on wave propagation in the plasma. This is the first time this has been demonstrated in a computer simulation of a plasma. Most previous computer simulation studies of plasmas were done under the assumption that the plasma boundaries could be neglected and the plasma was therefore considered to be infinite.

Figures 4.6(b) and 4.8(b) show the variation of the wave amplitude (squared) across the system for the Dattner mode with the highest cutoff frequency and normalized propagation constants of $\beta d = 6.357$ and $\beta d = 12.71$. One can observe that the energy propagating in the Dattner modes is primarily within the plasma itself and virtually nonexistent outside the plasma. This is in sharp contrast to the behavior of

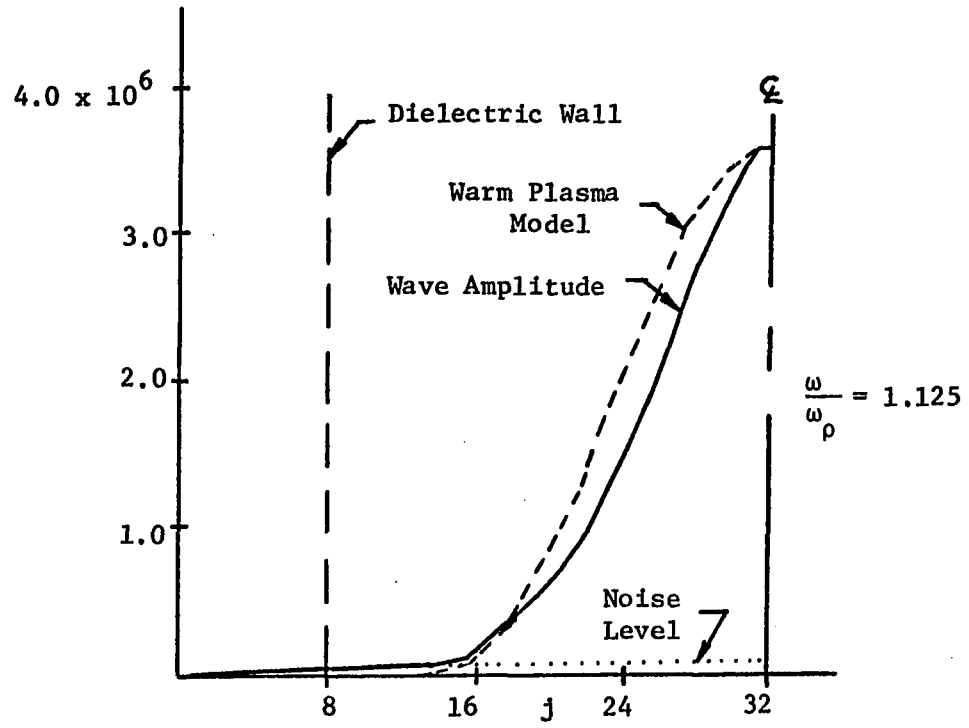

(b)

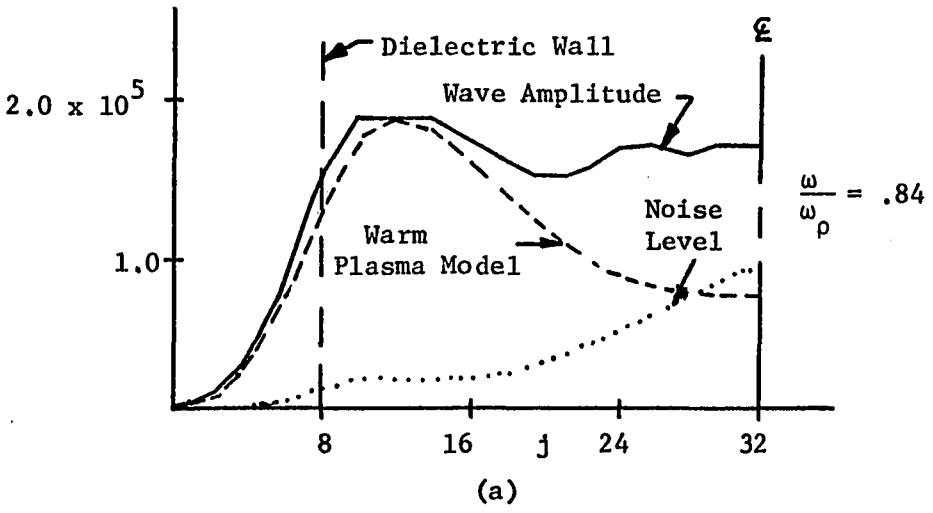

(a)

Fig. 4.6 Variation of Wave Amplitude (squared) Across the System for the Symmetric Simulation, βd = 6.357

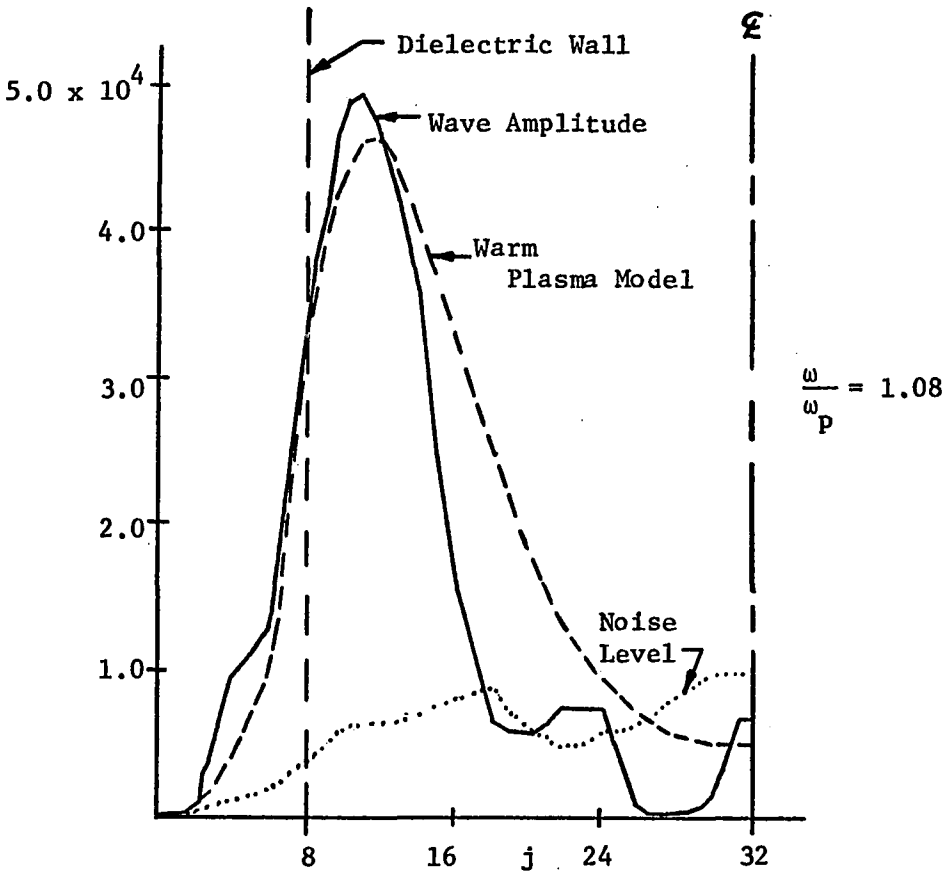

Fig. 4.7 Variation of Surface Wave Mode Amplitude (squared) Across the System for the Symmetric Simulation, $\beta d = 12.71$

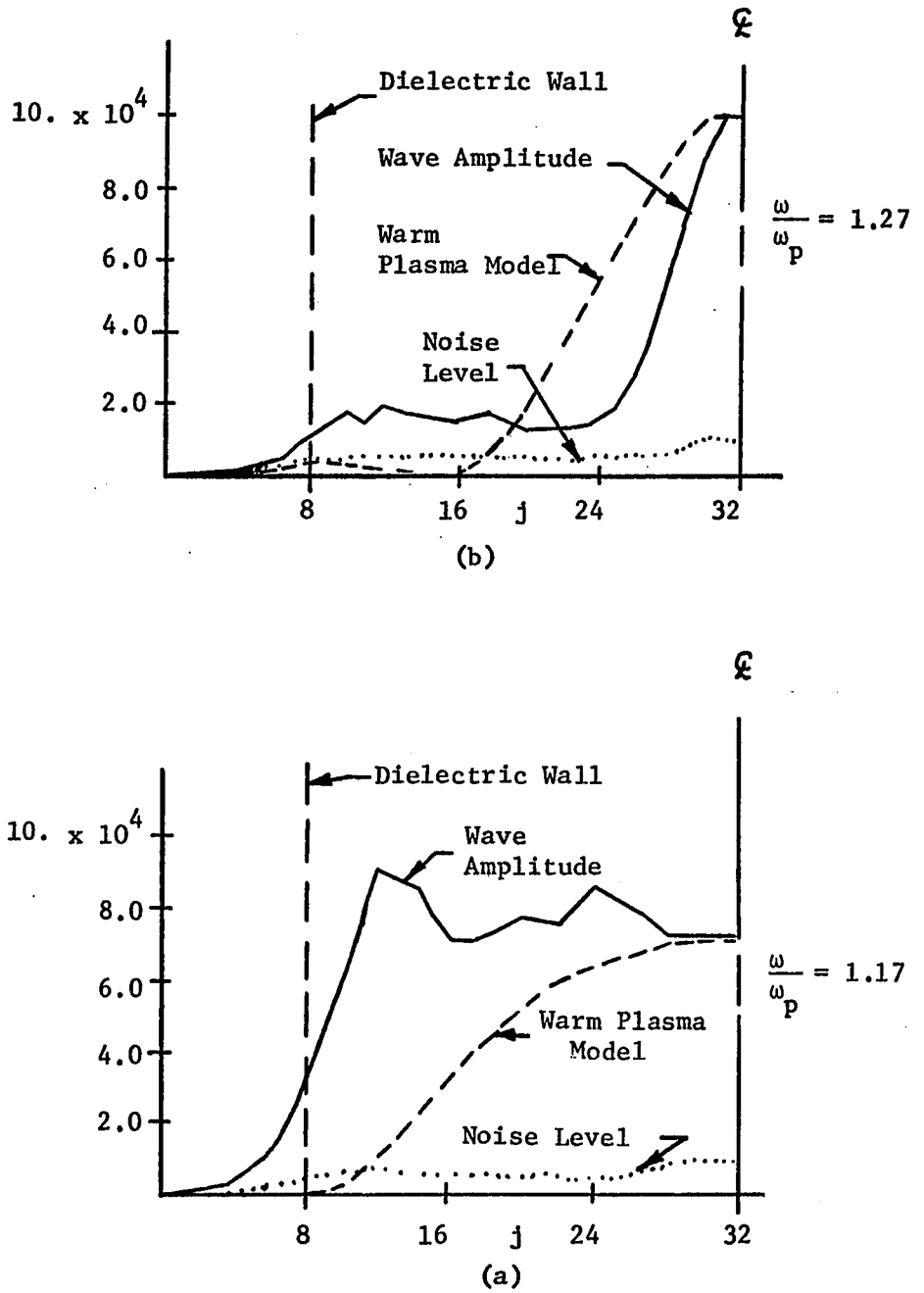

Fig. 4.8 Variation of Dattner Mode Wave Amplitude (squared) Across the System for the Symmetric Simulation, $\beta d = 12.71$

surface wave modes where the energy is stored at the dielectric-plasma boundary in the dielectric as well as the plasma. The qualitative agreement between the computer simulation model and the warm plasma model results are good.

Figure 4.8 shows the transverse variation of the wave amplitude (squared) for the Dattner mode with the lower cutoff frequency. Again, one observes that the energy in the wave is predominately within the plasma. The plasma simulation model predicts that this energy extends over a greater portion of the plasma than does the warm plasma model.

The computer simulation model results are in good agreement with the results obtained using the warm plasma model. This computer simulation model is a very general model. Its application to other problems requires only minor changes to the existing simulation program. Lastly, the computer simulation model is not a linearized model. It is applicable to the investigation of nonlinear phenomena just as well as it is to linear phenomena.

The Inhomogeneous Plasma

A major advantage of the computer simulation model of a plasma is its ease of extension to more difficult problems. As an example, consider the inhomogeneous plasma case. Equation (2.33) may be solved for the steady state electron density in an inhomogeneous plasma. One obtains

$$n_o = n_{eo}\, e^{q\phi_o/k_B T} \tag{4.7}$$

where n_{eo} is the electron density on the centerline of the system where the potential is taken to be zero for convenience. The steady state potential is produced by the surface charge on the boundary. Its purpose is to contain the electrons within the plasma. The steady state potential forms a potential well which holds the electrons. We shall consider the case of a parabolic potential well. The potential is given by

$$\phi_o = -\alpha Z'^2 \tag{4.8}$$

where Z' is the distance from the centerline of the system. The ion density is computed from the electron density using Poisson's equation as

$$n_i(Z') = \frac{2\alpha\varepsilon_o}{q} + n_o \tag{4.9}$$

The average electron density is given by

$$\langle n_o \rangle = \frac{n_{eo}}{2a} \int_{-a}^{a} e^{-q\alpha Z'^2/k_B T}\, dZ' \quad . \tag{4.10}$$

The total number of electrons per unit length is

$$\int_{-a}^{a} n_o(Z')dZ' \tag{4.11}$$

and the total number of ions per unit length is

$$\int_{-a}^{a} n_i(Z')dZ'dZ' = \int_{-a}^{a} \frac{2\alpha\varepsilon_o}{q} dZ' + \int_{-a}^{a} n_o dZ'$$

$$= \frac{4a\alpha\varepsilon_o}{q} + \int_{-a}^{a} n_o dZ' \quad . \tag{4.12}$$

The excess positive charge per unit length is

$$q\left\{\int_{-a}^{a} n_i dZ' - \int_{-a}^{a} n_o dZ'\right\} = 4a\ \alpha\varepsilon_o \ . \tag{4.13}$$

Since the net charge per unit must be zero, there must be a negative surface charge on each wall. The value of the surface charge is

$$\sigma_w = -2a\ \alpha\varepsilon_o \quad . \tag{4.14}$$

It is the presence of this surface charge that causes the plasma to be inhomogeneous. This surface charge is immobile and creates a d.c. electric field which retards the steady state flow of electrons toward the walls and enhances that of the ions. The total electric field acting on an electron in the plasma is the sum of two components. The first component is the d.c. field component due to the surface charge on the wall and the space charge imbalance in the bulk of the plasma, and the second component of the electric field is the time varying component due to the presence of waves in the plasma. For the computer simulation model of the inhomogeneous plasma the electrons are initially distributed in space according to Eq. (4.7) and (4.8), and the ions are

distributed according to Eq. (4.9). The electrons are initially given velocities in a Maxwellian distribution and the ions are motionless throughout the simulation. Poisson's equation is solved each time step for the potential at every mesh point. The electric field is calculated from this potential. This electric field is not the total electric field in the system since the surface charge on the wall was not included in the charge distribution for the solution of Poisson's equation. The electric field calculated in this manner is due to the d.c. bulk charge density imbalance and the presence of waves in the plasma. The d.c. field due to the surface charge must be added to the field calculated from Poisson's equation to obtain the total electric field acting in the system. The magnitude of the component of the electric field due to the surface charge is $2\alpha a$ and its sense is toward the wall.

The value of α was chosen to be $1.x10^6$ for the computer simulation of the inhomogeneous plasma. This value of α is large enough to cause a significant inhomogeneity in the plasma. This value of α is also small enough so that there are still several electron rods per Debye square in the region adjacent to the plasma boundary. The steady state electron density profile is shown in Fig. 4.9. The electron density has been normalized to its value on the centerline of the system, n_{eo}. The computer simulation was carried out for 1500 steps with each time step being 1/30 of a plasma period. Figure 4.10 shows the data obtained from the inhomogeneous plasma simulation. $\langle\omega_p\rangle$ is the plasma frequency computed using the average electron density

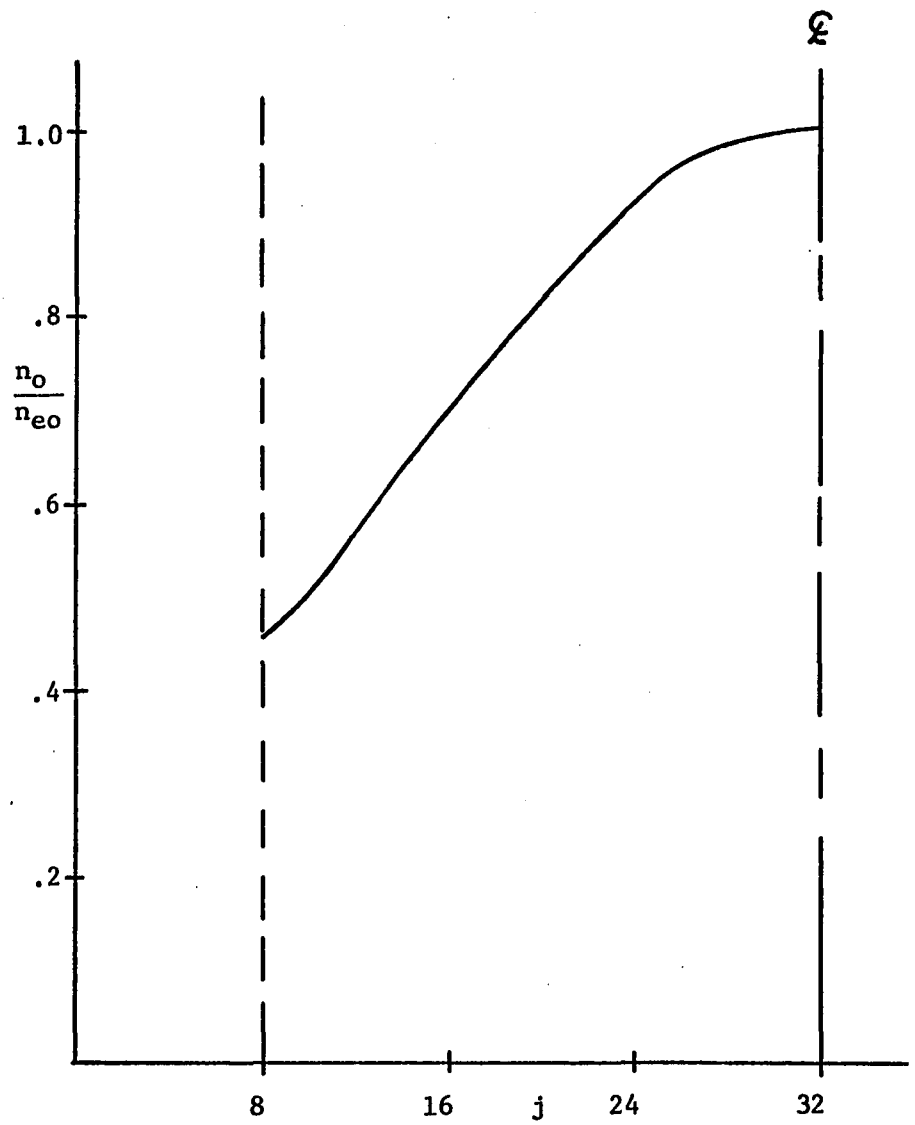

Fig. 4.9 Electron Density Profile for the Inhomogeneous Plasma Simulation

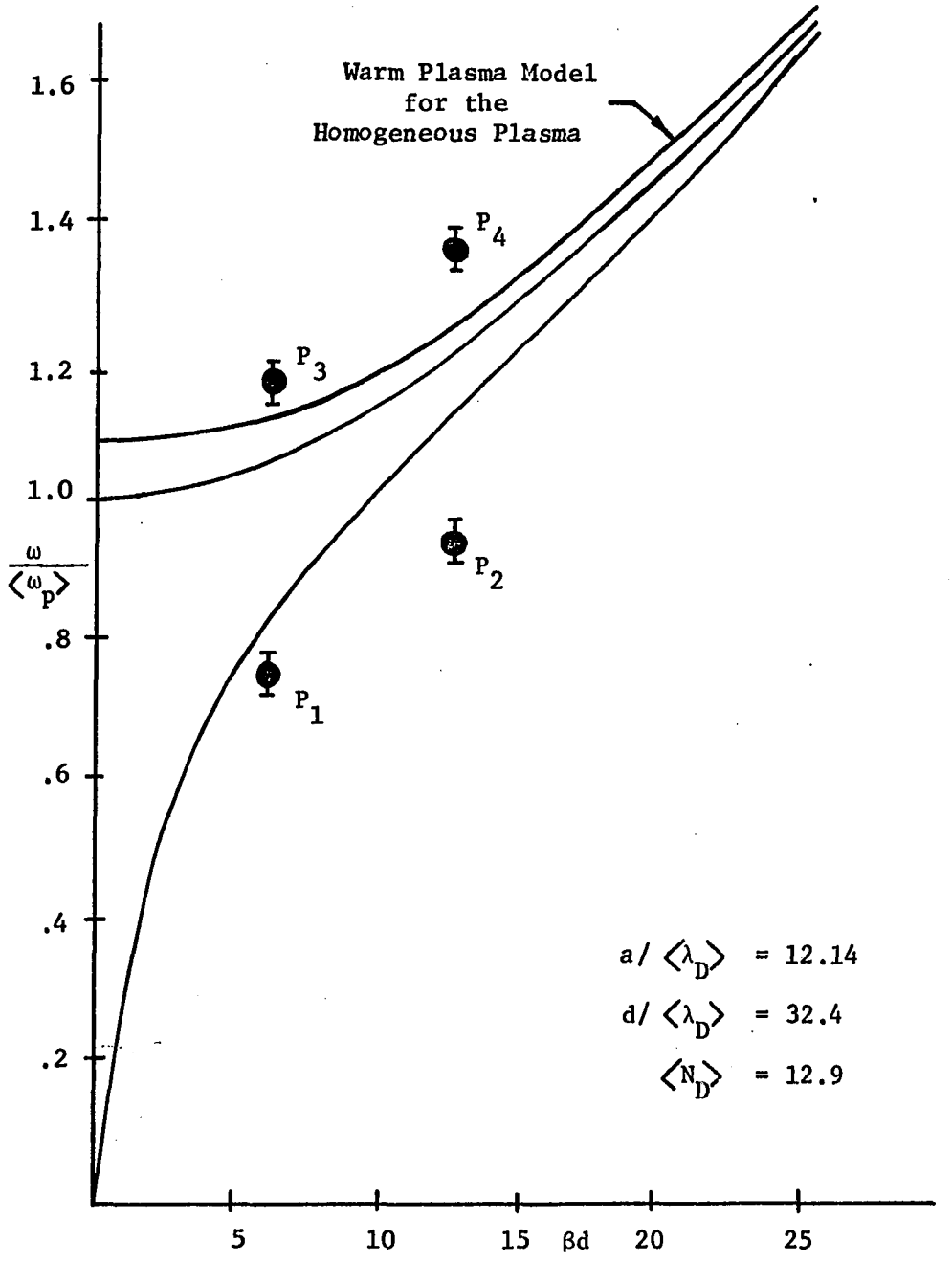

Fig. 4.10 ω-β Data from the Inhomogeneous Plasma Simulation

as given by Eq. (4.10). $\langle\lambda_D\rangle$ is the Debye length computed with the same average electron density. $\langle N_D\rangle$ is the average number of electron rods per $\langle\lambda_D\rangle$ square. Figures 4.11 and 4.12 show the variation of the wave amplitude (squared) across the system. The points p_3 and p_4 have their wave energy concentrated in the center of the plasma as is shown in Fig. 4.12. As has been discussed, this behavior is characteristic of the Dattner modes. Figure 4.11 shows that the points p_1 and p_2 have their wave energy concentrated at the plasma-dielectric interface. This identifies these two points as being the surface wave mode. Once again, it may be observed that as the propagation constant increases the wave energy becomes more tightly bound to the plasma-dielectric interface. If one compares these two data points with the similar points obtained in the homogeneous simulation, one finds that the inhomogeneous data is lower in frequency. This is to be expected since the surface wave energy is not distributed uniformly throughout the plasma, but is concentrated primarily at the edge of the plasma. As was discussed in Chapter 2, the frequency of the surface wave approaches $\omega_p/(1+\varepsilon_r)^{1/2}$ for intermediate values of β. In the inhomogeneous plasma ω_p decreases toward the plasma boundary. Because the energy of the surface wave is concentrated near this boundary, the surface wave effectively only sees this portion of the plasma. As β increases the portion of the plasma seen by the surface wave decreases and its frequency approaches $\omega_p/\sqrt{2}$. Since ω_p decreases toward the plasma boundary, the asymptotic value which the frequency approaches also decreases. This causes the frequency of the wave to be lower

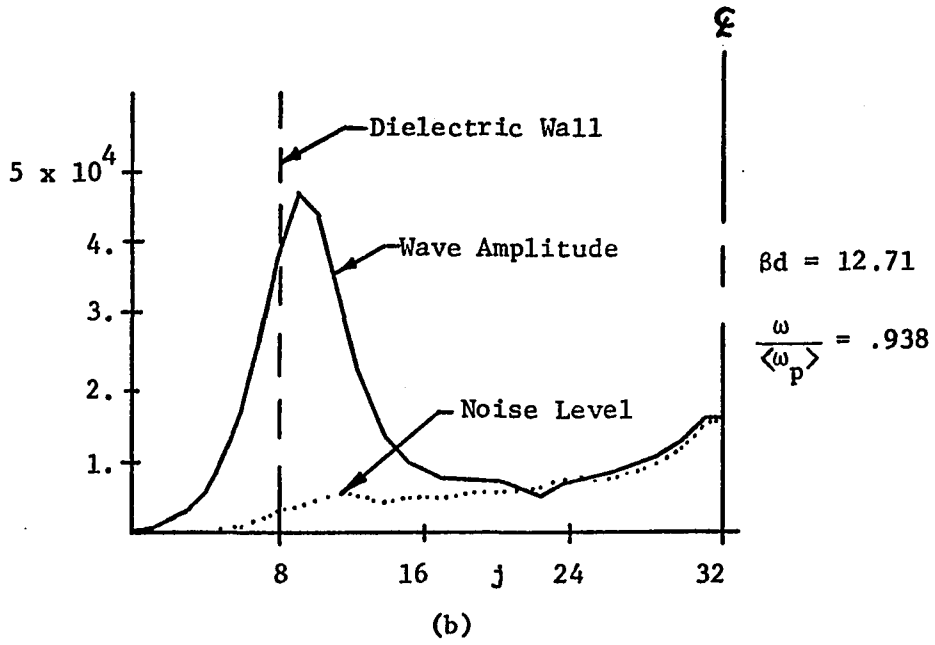

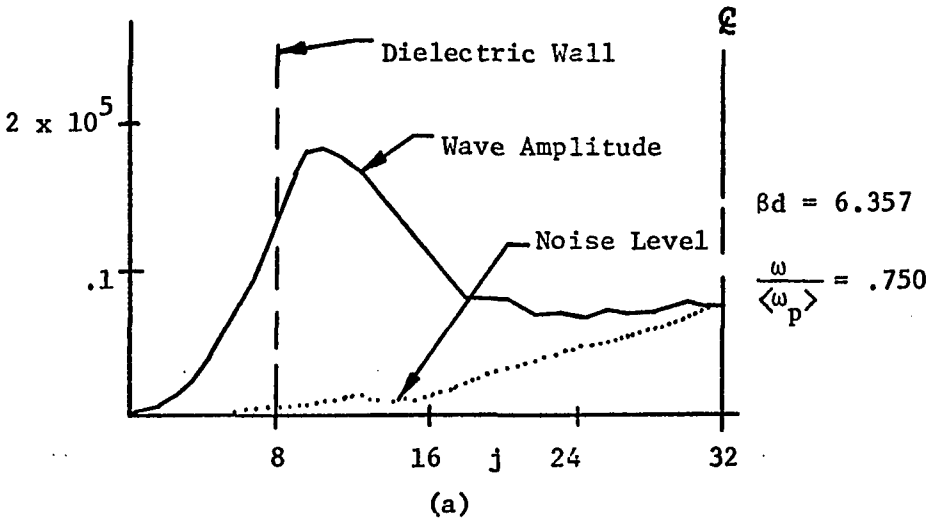

Fig. 4.11 Variation of Wave Amplitude (squared) Across the System for the Inhomogeneous Plasma Simulation

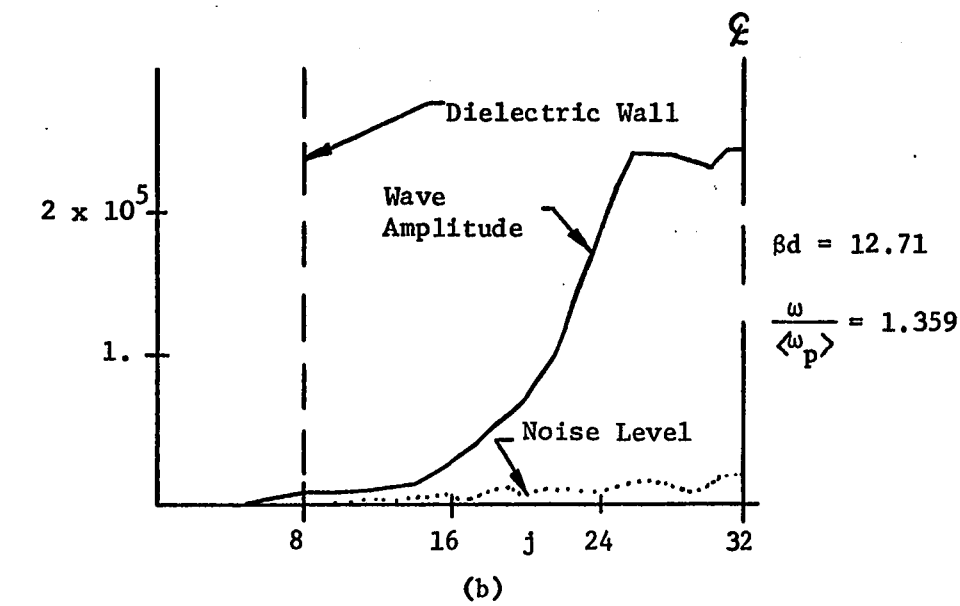

(b)

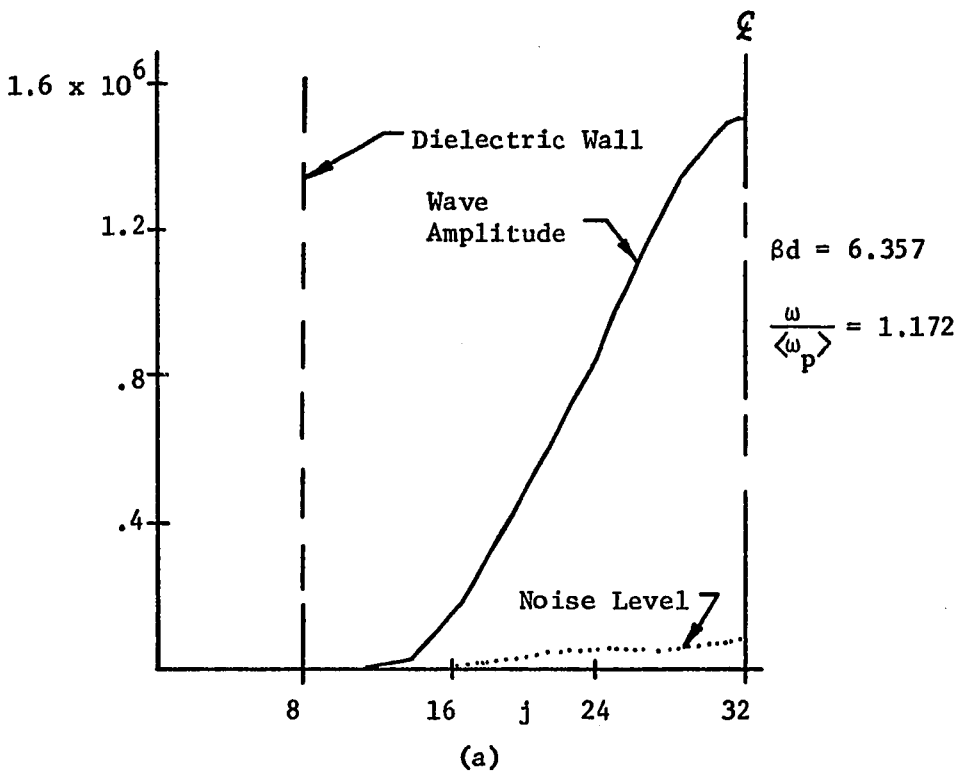

(a)

Fig. 4.12 Variation of Wave Amplitude (squared) Across the System for the Dattner Modes in the Inhomogeneous Plasma Simulation

than it would be if the plasma were homogeneous. This effect has been demonstrated theoretically and experimentally by Carlile and Swinford [1968].

The inhomogeneous plasma data was obtained by making the previously discussed changes to the same program that was used for the homogeneous plasma. The changes to the computer program were of the minor nature and so the extension of the computer simulation model of a plasma to the inhomogeneous plasma is fairly simple. This is to be contrasted with the difficulties in solving Eq. (2.37) in the case of the warm plasma model. This flexibility of the computer simulation model of the plasma is one of its greatest advantages.

CHAPTER 5

CONCLUSION

Summary

A computer simulation model has been developed to study wave propagation in a bounded thermal plasma. The model has been used to study the natural modes of this system, the surface wave modes and the Dattner modes. The importance of the plasma boundary on wave propagation in computer simulation studies of plasma has been demonstrated for the first time. Good agreement was found between the results of the computer simulation model and the predictions of the warm plasma model.

Suggestions for Further Work

Hockney [1968] found that by coding portions of his Poisson solver program, POT1, in the assembly language of the computer (COMPASS on the CDC 6400 computer) he could obtain execution speeds which were 5.7 times faster than the times obtained from the all-FORTRAN version of the program. By coding other sections of the computer simulation program in the machine assembly language one would expect to be able to reduce the time of a simulation step by a similar factor. This would be particularly important in the operations which are repeated every time step such as the computation of charge density and the acceleration and movement of the electron rods as well as the

computation of the electric potential. Coding these sections of the simulation program in the machine assembly language would result in a significant reduction in the cost of computer simulation of plasma.

The central memory size of the University of Arizona's CDC 6400 computer limits one to the use of only 5000 electron rods. To study larger systems, however, one needs to use more electron rods. This might be economically accomplished by developing a machine assembly language sub-program to store the x and y components of an electron rod's velocity in a single computer central memory word. The x and y components of the electron rod's position could be stored in a second central memory word. This would mean that only two central memory words would be required to specify the state of an electron rod instead of the present four words. One could then use twice as many electron rods.

An important extension of the present work would be to the nonlinear regime. In this case a given mode is driven by an externally applied field at the frequency and propagation constant of the mode and the growth of the wave and the subsequent heating of the plasma are studied. Engineering applications such as this are ideal for a plasma simulation model and the results would be of some significance in the controlled thermonuclear effort.

REFERENCES

Akao, Y., and Y. Ida. Journal of Applied Physics, Vol. 35, No. 9, September, 1964, p. 2565.

Birdsall, C. K. Physics of Fluids, Vol. 13, No. 8, August, 1970, p. 2115.

Birdsall, C. K., and D. Fuss. Journal of Computational Physics, Vol. 3, 1969, p. 494.

Buneman, O. Journal of Computational Physics, Vol. 1, No. 4, June, 1967, p. 517.

Carlile, R. N. Internal Technical Memorandum No. TM-30, University of California, Berkeley, California, 1963.

Carlile, R. N., and H. W. Swinford. Journal of Applied Physics, Vol. 39, No. 7, June, 1968, p. 3268.

Crawford, F. W. IEEE Transactions on Nuclear Science, NS-11, January, 1964, p. 12.

Dattner, A. Ericson Technics, Vol. 2, 1963, p. 309.

Dawson, J. M. Physics of Fluids, Vol. 5, No. 4, April, 1962, p. 445.

Dawson, J. M. Physics of Fluids, Vol. 7, No. 3, March, 1964, p. 419.

Dawson, J. M. Conference on Numerical Simulation of Plasma, Las Alamos Scientific Laboratory, Las Alamos, New Mexico, September 18-20, 1968.

Delcroix, J. L. Plasma Physics, John Wiley and Sons, New York, 1965.

Diament, P., V. L. Granatstein, and S. P. Schlesinger. Journal of Applied Physics, Vol. 37, No. 3, March, 1966, p. 1771.

Granatstein, V. L., and S. P. Schlesinger. Journal of Applied Physics, Vol. 36, No. 11, November, 1965, p. 3503.

Hockney, R. W. Technical Report SUIPR No. 53, Stanford University, Stanford, California, May, 1966.

Hockney, R. W. Technical Report SUIPR No. 202, Stanford University, Stanford, California, October, 1967.

Hockney, R. W. Conference on Numerical Simulation of Plasma, Las Alamos Scientific Laboratory, Las Alamos, New Mexico, September 18-20, 1968.

Kruer, W. L., and J. M. Dawson. Third Annual Numerical Plasma Simulation Conference, Stanford University, Stanford, California, September 2-5, 1969.

Kunkel, W. B. Plasma Physics in Theory and Application, McGraw-Hill, New York, 1966.

O'Brien, B., R. W. Gould, and J. Parker. Physical Review Letters, Vol. 14, No. 16, April 19, 1965, p. 630.

Okuda, H. Third Annual Numerical Plasma Simulation Conference, Stanford University, Stanford, California, September 2-5, 1969.

Parker, J. V., J. C. Nickel, and R. W. Gould. Physics of Fluids, Vol. 7, No. 9, September, 1964, p. 1489.

Rommell, D. Nature, Vol. 167, February 10, 1951, p. 243.

Tonks, L. Physical Review, Vol. 37, No. 6, June, 1931, p. 1458.

Trivelpiece, A. W. Technical Report No. 7, California Institute of Technology, Pasadena, California, May, 1958.